



## Characterisation of Ground Thermal and Thermo-Mechanical Behaviour for Shallow Geothermal Energy Applications

Ana Vieira, João Maranha, Paul Christodoulides, Maria Alberdi-Pagola, Fleur Loveridge, Frédéric Nguyen, Georgios Florides, Georgia Radioti, Francesco Cecinato, Iulia Prodan, et al.

### ► To cite this version:

Ana Vieira, João Maranha, Paul Christodoulides, Maria Alberdi-Pagola, Fleur Loveridge, et al.. Characterisation of Ground Thermal and Thermo-Mechanical Behaviour for Shallow Geothermal Energy Applications. *Energies*, 2017, 10 (12), <10.3390/en10122044>. <hal-01717735>

**HAL Id: hal-01717735**

**<https://hal.science/hal-01717735v1>**

Submitted on 7 Mar 2018

**HAL** is a multi-disciplinary open access archive for the deposit and dissemination of scientific research documents, whether they are published or not. The documents may come from teaching and research institutions in France or abroad, or from public or private research centers.






L'archive ouverte pluridisciplinaire **HAL**, est destinée au dépôt et à la diffusion de documents scientifiques de niveau recherche, publiés ou non, émanant des établissements d'enseignement et de recherche français ou étrangers, des laboratoires publics ou privés.



Distributed under a Creative Commons CC BY 4.0 - Attribution - International License

Review

# Characterisation of Ground Thermal and Thermo-Mechanical Behaviour for Shallow Geothermal Energy Applications

Ana Vieira <sup>1</sup> , Maria Alberdi-Pagola <sup>2</sup>, Paul Christodoulides <sup>3</sup> , Saqib Javed <sup>4</sup>, Fleur Loveridge <sup>5,\*</sup> , Frederic Nguyen <sup>6</sup>, Francesco Cecinato <sup>7</sup>, João Maranhã <sup>1</sup>, Georgios Florides <sup>3</sup>, Iulia Prodan <sup>8</sup>, Gust Van Lysebetten <sup>9</sup>, Elsa Ramalho <sup>10</sup>, Diana Salciarini <sup>11</sup>, Aleksandar Georgiev <sup>12</sup>, Sandrine Rosin-Paumier <sup>13</sup> , Rumen Popov <sup>14</sup>, Stanislav Lenart <sup>15</sup> , Søren Erbs Poulsen <sup>16</sup> and Georgia Radioti <sup>6</sup>

- <sup>1</sup> Geotechnics Department-National Laboratory for Civil Engineering, 1700-066 Lisbon, Portugal; avieira@lnec.pt (A.V.); jmaranha@lnec.pt (J.M.)
  - <sup>2</sup> Department of Civil Engineering, Aalborg University, Aalborg 9000, Denmark; mapa@civil.aau.dk
  - <sup>3</sup> Faculty of Engineering and Technology, Cyprus University of Technology, 3036 Limassol, Cyprus; paul.christodoulides@cut.ac.cy (P.C.); georgios.florides@cut.ac.cy (G.F.)
  - <sup>4</sup> Building Services Engineering, Lund University, Lund 22100, Sweden; saqib.javed@hvac.lth.se
  - <sup>5</sup> School of Civil Engineering, University of Leeds, Leeds LS2 9JT, UK
  - <sup>6</sup> Urban and Environmental Engineering, University of Liege, 4000 Liege, Belgium; f.nguyen@uliege.be (F.N.); gradioti@uliege.be (G.R.)
  - <sup>7</sup> Department of Civil, Environmental and Mechanical Engineering, University of Trento, 38123 Trento, Italy; francesco.cecinato@unitn.it
  - <sup>8</sup> Faculty of Civil Engineering, Technical University of Cluj-Napoca, Constantin Daicoviciu Street, No.15, Cluj-Napoca 400020, Romania; iulia.prodan@dst.utcluj.ro
  - <sup>9</sup> Belgian Building Research Institute, 1342 Limelette, Belgium; gust.van.lysebetten@bbri.be
  - <sup>10</sup> Laboratório Nacional de Energia e Geologia, 2610 Amadora, Portugal; elsa.ramalho@lneg.pt
  - <sup>11</sup> University of Perugia, Department of Civil and Environmental Engineering, 06125 Perugia, Italy; diana.salciarini@unipg.it
  - <sup>12</sup> Department of Mechanics, Technical University of Sofia, Plovdiv Branch, 4000 Plovdiv, Bulgaria; ageorgiev@gmx.de
  - <sup>13</sup> Université de Lorraine, LEMTA, CNRS, UMR 7563, F-54500 Vandoeuvre-lès-Nancy, France; sandrine.rosin@univ-lorraine.fr
  - <sup>14</sup> EKIT Department of Plovdiv University “Paisii Hilendarski”, 4000 Plovdiv, Bulgaria; rum\_pop@yahoo.com
  - <sup>15</sup> Slovenian National Building and Civil Engineering Institute, 1000 Ljubljana, Slovenia; stanislav.lenart@zag.si
  - <sup>16</sup> Centre of Applied Research and Development-Building, Energy and Environment, VIA University College, 8700 Horsens, Denmark; soeb@via.dk
- \* Correspondence: f.a.Loveridge@leeds.ac.uk; Tel.: +44-11-3343-0000

Received: 3 October 2017; Accepted: 21 November 2017; Published: 3 December 2017

**Abstract:** Increasing use of the ground as a thermal reservoir is expected in the near future. Shallow geothermal energy (SGE) systems have proved to be sustainable alternative solutions for buildings and infrastructure conditioning in many areas across the globe in the past decades. Recently novel solutions, including energy geostructures, where SGE systems are coupled with foundation heat exchangers, have also been developed. The performance of these systems is dependent on a series of factors, among which the thermal properties of the soil play a major role. The purpose of this paper is to present, in an integrated manner, the main methods and procedures to assess ground thermal properties for SGE systems and to carry out a critical review of the methods. In particular, laboratory testing through either steady-state or transient methods are discussed and a new synthesis comparing results for different techniques is presented. In situ testing including all variations of the thermal response test is presented in detail, including a first comparison between new and traditional approaches. The issue of different scales between laboratory and in situ measurements is

then analysed in detail. Finally, the thermo-hydro-mechanical behaviour of soil is introduced and discussed. These coupled processes are important for confirming the structural integrity of energy geostructures, but routine methods for parameter determination are still lacking.

**Keywords:** shallow geothermal systems; soil thermal behaviour; laboratory testing; in situ testing; thermo-mechanical behaviour

---

## 1. Introduction

The use of renewable energy sources ranks significantly on the political agenda in many countries. Development is also associated with efficient energy management. The implementation of new renewable energy technologies has increased significantly in recent years and the development of this sector is in constant growth. Shallow geothermal energy (SGE) applications for buildings and infrastructure conditioning are being increasingly used. Exploitation of the subsurface top layers as a thermal reservoir is already common practice in many countries. The development of geothermal technology so that it can become a significant energy resource towards a 100% renewable heating and cooling scenario is a target in Europe by 2030 [1].

SGE systems may take a number of different forms [2]. All systems have some type of ground heat exchanger (GHE), connected to a heat delivery system, usually via a heat pump. Traditional forms of GHE include borehole heat exchangers, in which pipes for the circulation of a heat transfer fluid are embedded into small diameter boreholes up to 200 m deep, and shallower horizontal systems in which the pipes are arranged in trenches near the ground surface. The former is typically used where available space is restricted. However, novel types of heat exchangers are now routinely being developed, with energy geostructures being constructed in a number of countries [3]. These types of GHEs make dual use of civil engineering structures such as piled foundations, retaining walls, and tunnels [4], so that they serve as heat exchangers in addition to providing structural support.

The thermal efficiency of SGE systems depends on a number of factors including the type of GHE [5,6], its thermal properties [7,8], the thermal behaviour of the surrounding ground [9,10], and the thermal demand [11]. Trends to increase thermal efficiency include ensuring heat transfer pipe separation and engineering thermally enhanced grouting material. Additionally, for energy geostructures, it is important to understand the thermo-hydro-mechanical behaviour of the ground since temperature changes during GHE operation can lead to the development of resulting changes in stress and strain in the structure [12]. These changes need to be evaluated to ensure that there is no detrimental impact on the structural performance of the energy geostructure.

This paper considers the important topic of determination of the ground thermal properties, either in situ or in the laboratory, since without accurate information designs may over- or underestimate energy availability or incorrectly assess structural integrity. The focus is on the key thermal properties of ground thermal conductivity and GHE thermal resistance, which govern energy assessment, and on understanding the nature of the thermo-hydro-mechanical behaviour. Presenting information on techniques to obtain this information together in a unified form for the first time will provide a unique resource for scholars and practitioners in energy geostructures and other SGE systems.

The paper is organised in sections that contain critical reviews of a topic area. Section 2 provides an outline of the thermal and thermo-hydro-mechanical (THM) processes that occur in the ground. Section 3 focuses on laboratory testing for soil and rock thermal conductivity, bringing new insights into the differences between different testing techniques. Section 4 considers in situ thermal response testing for thermal conductivity and GHE thermal resistance, including a review of recent advances in the technique. Section 5 studies the differences in thermal properties that can be obtained at different scales, and Section 6 reviews approaches for determining thermo-hydro-mechanical properties relevant

for soil behaviour. Finally, Section 7 summarises the key points and provides recommendations of the most appropriate techniques.

## 2. Thermo-Hydro-Mechanical Processes in Soil and Rocks

The three main heat transfer processes can all occur in soils and rocks: conduction, convection, and radiation. However, conduction is usually the dominant process [13] and hence will be the main focus of Sections 3–5 of this paper. Fourier's law is the basic law that describes thermal conduction. Its differential form written for heat transfer in one direction is (e.g., [14]):

$$Q = -\lambda A \frac{\partial T}{\partial x} \quad (1)$$

where  $Q$  is the heat flow rate in the  $x$ -direction (W);  $\lambda$  is the thermal conductivity, a property of the material ( $\text{W}\cdot\text{m}^{-1}\cdot\text{K}^{-1}$ );  $A$  is the area normal to the direction of heat flow ( $\text{m}^2$ ); and  $\partial T/\partial x$  is the temperature gradient ( $\text{K}\cdot\text{m}^{-1}$ ). The main factors that influence soil or rock bulk thermal conductivity are the properties of the different phases (solid, pore fluid, pore air), usually measured in terms of density and moisture content. Consequently, empirical prediction models for soil thermal conductivity have historically been used (e.g., [15–19]). However, these can lead to significant errors [13] and do not account for factors such as soil structure, heterogeneity, and anisotropy, which might become important [20].

For soils, Figure 1 illustrates the situations where convection and radiation may also occur and become significant. Understanding the types of soils and conditions susceptible to these additional thermal processes is important, since their occurrence may lead to errors in property determination and, consequently, in the later system design. This will be discussed in Sections 3 and 5 of the paper.

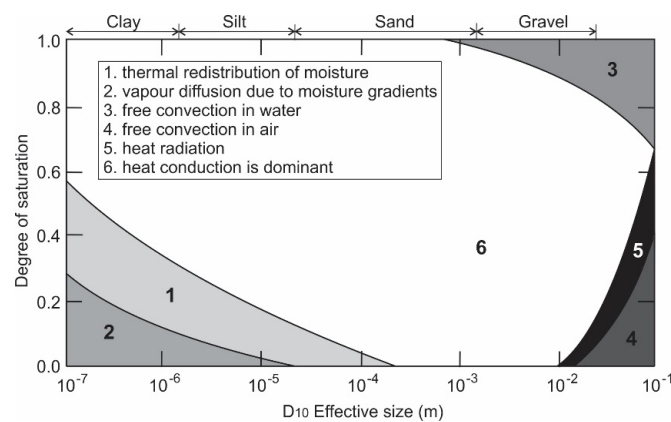


Figure 1. Main heat transfer processes in soils (after [19]).

Hellstrom [21] suggests that SGE system performance can be affected by free convection if the hydraulic conductivity of the soil is greater than around  $10^{-5}$  m/s in both vertical and horizontal directions. However, in most cases, soil and rock stratification reduces the vertical permeability or introduces less permeable horizons, which would be a significant barrier to this process. In soils and rocks, forced convection is typically more significant and occurs if ground water is flowing. It can be particularly important in fractured rocks, where thermal dispersion can also play a role [22].

The movement of moisture may be important in fine grained unsaturated soils [19]. Heating processes can cause pore water evaporation, as the water absorbs the energy associated with the latent heat of evaporation. The water vapour will then be susceptible to vapour pressure gradients and it will migrate through the soil to an area of lower vapour pressure. Here, the temperature may also be lower and the vapour would then condense, releasing the latent heat in a new location. In addition to making a contribution to the heat transfer process, moisture migration also changes the thermal



properties of the soil by affecting phase proportions. With high temperature gradients resulting from heat injection, drying of the soil can reduce the thermal conductivity. Hellstrom [21] suggests that this phenomenon becomes significant in high porosity soils of low saturation when temperatures surpass 25 °C. Consequently, this phenomenon is being considered in current research (e.g., [12]).

Moisture migration is one example of thermo-hydraulic coupling of soil behaviour. However, with the introduction of energy geostructures, it becomes important to consider how thermal loading affects not just the hydraulic conditions, but also the mechanical ones. The magnitude of these effects and the way they evolve with time should be taken into account and quantified to achieve a sustainable design. To this aim, multi-physical analysis, namely coupled thermo-hydro-mechanical (THM) analysis, should be ideally undertaken.

The effect of temperature in the mechanical behaviour of soils is well-known and rather complex, and has been confirmed for decades in a number of experimental tests (e.g., [23–26]). For SGE applications this is essentially a one-way effect, as the influence of mechanical actions on the temperature field is usually negligible (Figure 2). On the contrary, the thermal and hydraulic effects are mutually coupled, thereby thermal loads may induce changes in pore pressures and in the water flow regime, and the hydraulic conditions may also affect the thermal field (since the pore fluids conduct and transport heat). Lastly, the mechanical and hydraulic effects also exhibit mutual interaction, caused by changes in effective stress induced by pore pressure variations.

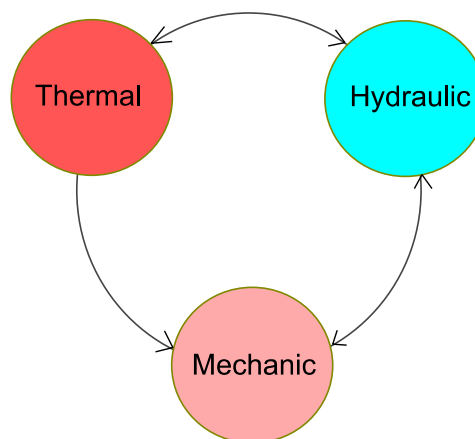


**Figure 2.** Schematic representation of relevant couplings in shallow geothermal energy (SGE) systems.

### 3. Laboratory Thermal Testing of Soils and Rocks

The thermal conductivity of soils and rocks can be determined by laboratory measurements that are cheaper and usually quicker than in situ tests. However, laboratory measurements do not account for site-specific conditions such as the presence of high groundwater flow, spatial heterogeneity, and scale effects that directly impact the effective thermal properties (see Section 5).

In general, steady-state and transient methods can be used for thermal conductivity testing. The steady-state methods determine thermal properties by establishing a temperature difference across the sample that does not change with time, while transient methods monitor the time-dependent heat dissipation within a sample.

The variation of the water content and the destructuration of soil due to the sampling operation can also have a major impact on the evaluation of thermal properties. Furthermore, thermal conductivity is an anisotropic property in soils and rocks, and this should also be considered in testing programmes.

The remainder of this section presents a review of the most commonly used methods for assessing the thermal conductivity of soils. This is followed by a comparison of the different techniques with a critical review.

### 3.1. Steady-State Methods

Steady-state techniques perform a measurement when the temperature of the material measured does not change with time. This makes the analysis straightforward since Fourier's Law can be applied directly. The disadvantage is that a well-engineered experimental setup is usually needed.

Typical characteristics of steady-state methods are long measurement times (hours to days for single data points), and complicated apparatus and controls to create and maintain the desired heat flows. The measurements are taken at a mean temperature between the hot and cold ends of a sample and there may be difficulties due to contact resistances [27].

#### 3.1.1. Absolute Techniques

The basic principle of the steady-state absolute technique is shown in Figure 3a. In principle, a heat source supplies a steady heat flow ( $Q$ ) at one surface of a sample that is transferred through the sample volume to its opposite side, where a heat sink is present. Ideally, no heat leakage should occur from the source, the specimen, or the boundaries, thus ensuring a one-dimensional (1D) thermal heat flow in the test section. The temperature ( $T_1$ ) of the heater and that of the heat sink ( $T_2$ ), after an initial stage, are constant and are monitored by a control system. There are many apparatus variants on the absolute method. The key approaches for soils and rocks are described below.

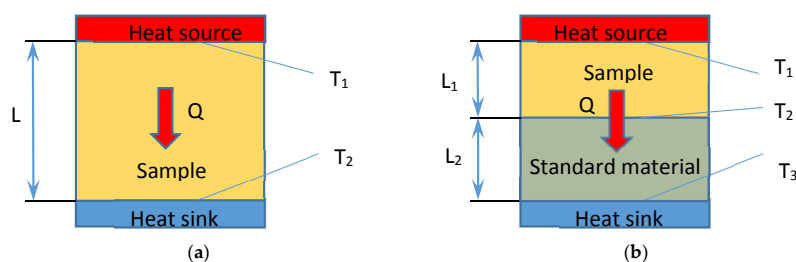


**Figure 3.** Principles of steady state methods (a) Absolute technique; (b) Configuration of the comparative cut-bar technique.

A typical test apparatus of the absolute technique is the guarded hot plate apparatus [28–30]. The guards serve to minimise lateral heat losses, which could otherwise affect the accuracy of the method. The plates must be as flat as possible and should be made from a highly conductive material to ensure good uniformity of temperature across them. They should also have high emissivity surfaces, particularly when one is measuring low thermal conductivity materials. The temperature balance between the guards and the metering area must also be maintained within close limits (about 0.01 °C) to give confidence of negligible lateral heat exchange [31]. The sample tested needs to be relatively large (in the cm scale) and needs to be prepared in a standard circular or rectangular shape. Also, the testing time is usually long, in the range of a few hours [32].

While not explicitly designed with soils in mind, the guarded hot plate has been used for this application. In References [33,34] the thermal conductivity of sands was measured using this apparatus, while in Reference [35] the method was applied to clay soils. Similar approaches to the guarded hot plate are reported in the literature, such as the thermal cell that has been used for the measurement of clayey samples in Reference [36] and a wider range of soils in [37]. In Reference [38], the thermal cell of Reference [37] was further developed to reduce heat losses and hence improve accuracy.

The absolute technique is recognised as the most accurate technique for determining the thermal conductivity of insulation materials, having an uncertainty of about 1.5% over a limited, near ambient temperature range [31]. However, testing soils is more challenging since moisture migration in unsaturated soils can occur when carrying out long duration steady-state tests. Studies such as that in Reference [36] have also shown the importance of eliminating heat losses if accuracy is to be maintained. Therefore, overall lower than typical accuracy should be expected when testing soils.

### 3.1.2. Comparative Cut-Bar Technique

To avoid the uncertainty of the determination of the heat flow through the sample when using the absolute technique, the comparative technique can be used [39], also known as the divided cut-bar method. This method is an improvement of the absolute technique, where a standard material with known thermal conductivity is positioned in the line of heat flow, as shown in Figure 3b. In this way, the heat flow need not be measured since the amount of heat flow through the standard material is equal to that of the testing sample. The thermal conductivities  $\lambda_i$  of the test sample are then related by:

$$\lambda_1 = \lambda_2 \frac{A_2 L_1 (T_2 - T_3)}{A_1 L_2 (T_1 - T_2)} \quad (2)$$

$L_i$  is the length of the material,  $A_i$  is the area normal to the direction of heat flow, and  $T_i$  represents the corresponding temperatures ( $i = 1, 2, 3$ ), as shown in Figure 3b.

Results and accuracy depend on the same general parameters of the absolute method. The divided cut-bar has been used successfully to measure mainly rock samples, as in References [20,40]. Rock samples are much less prone to moisture migration and therefore, provided heat losses are controlled, the method is reliable.

## 3.2. Transient Methods

Transient, time, or frequency domain methods enable quick measurement of thermal conductivity as they do not need to wait for a steady-state. The measurements are usually performed during the modulated heating up process. The heating source can be either electrical or optical, while temperature can be measured by contact (e.g., thermocouple) or without contact (infrared). A large number of devices (particularly time domain methods) are commercially available, of which the most commonly used types for soils are reviewed below. Frequency domain methods, such as the  $3\omega$  method and the Frequency Domain Thermoreflectance Technique (FDTR), are highly accurate methods that, while used for other materials (e.g., [41]), are not generally applied to soils at present. This may be because those methods require a very smooth surface of the tested material.

### 3.2.1. Needle-Probe Method

Most laboratory measurements of soil thermal conductivity are made using a heated wire or needle probe modelled as a perfect line conductor. So-called transient probe methods may be described as follows: a body of known dimensions and thermal constants (the 'probe'), which contains a source of heat and a thermometer is immersed in the medium whose constants are unknown. With the aid of suitable theoretical relations, these constants are then deduced from a record of probe temperature versus elapsed time [42,43].

Different sizes and types of probes can be utilised. Standard needles are constructed with a minimum diameter of 2 mm and can vary to a diameter of about 6 mm and a length of 45 mm and longer [44,45]. For soft soils, the probes can be inserted directly into the material. For harder samples, predrilling may be required, with the use of contact fluid or guiding tubes inserted first (Figure 4). The minimum diameter of the sample, according to Reference [46], is 40 mm and its minimum length is the probe length plus 20%. For higher values of thermal conductivity, a larger sample size is necessary. The accuracy of the measurements is theoretically about 2–3% and the time of measurement depends on the thermal conductivity value, varying from a few minutes to about 20 min. Examples of applying such devices to soils/rocks can be found, e.g., in References [20,47].

Kasubuchi [48] developed the twin heat probe method, which is a comparative technique based on the thermal needle probe method. It was later used in Reference [35] for measuring clayey samples with good agreement against guarded hot plate data. Another advanced version of the thermal needle probe, which simultaneously provides thermal conductivity and thermal diffusivity, is the dual thermal needle probe by Reference [49]. Here, the thermal properties are determined from the temperature

collected by a receptor needle, over time at a known distance from a line heat source placed in a parallel needle. This method has been applied to soils in References [50,51]. The main disadvantage of this over the traditional single needle probe is the potential for change in the separation of the two needles when inserted into a soil sample, since any change at this distance will affect the subsequent calculations of thermal properties.

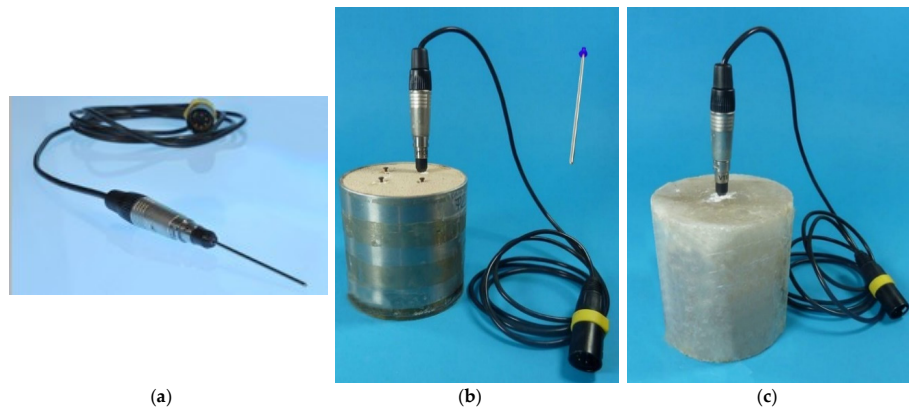


**Figure 4.** Transient probes and applications, modified from Reference [44]. (a) Each probe contains a heating device and a temperature sensor embedded in a stainless-steel case. The probes come pre-calibrated, ready for use with a computer monitoring and analysing system; (b) To determine the thermal conductivity of the compacted and completely dried material, four guiding tubes were inserted at the measuring positions. Insert: metal guiding tube; (c) To position the needle probe along the axis of the core sample, the salt block was predrilled and contact fluid was applied to the probe before inserting it.

Following principles similar to those of the needle-probe method, multi-needle probes have been developed, which enable the measurement of different soil properties within the same soil volumes [52–55].

### 3.2.2. Transient Plane Source (TPS) Method

These surface probes basically contain a ‘resistive element’ that can be used both as a heat source and a temperature sensor. The probe is placed in good contact with a flat and slightly polished surface of a sample and a transient heating signal is transmitted. By recording and analysing the rise or decay of the temperature with time, the thermal properties of the sample, i.e., the thermal conductivity, the thermal diffusivity, the volumetric heat capacity, and the temperature of the sample, can be obtained [56].

The probes require a plane and smooth surface and are therefore probably best suited for use with rocks. Surface probes are more appropriate than needle probes when one deals with materials that are very hard or brittle and present difficulties in their drilling for a narrow and long hole with a constant diameter.

As some pressure should be applied on the probe to ensure a good contact with the material, surface probes should not be used to test compressible materials. A minimum sample size is always required to avoid reflection of the propagating heat wave at the sample boundaries. When this happens, the reflection disturbs the reading of the temperature sensor within the test time and affects the measurement. Therefore, the sample size should be between 10% and 20% longer than the probe’s length. Typical minimum sample sizes (always depending on the specifications of the probe) are a thickness of about 20 mm, and a length varying between 50 and 90 mm.

The length of the heat pulse is chosen to be short enough so that the heating element can be considered to be in contact with an infinite or semi-infinite solid throughout the transient recording. This implies that the time of a transient recording must be short enough so that the outer boundaries of

the sample do not influence the temperature increase to any measurable extent. The physical formulation and analysis is based on the general theory of the transient plane source (TPS) technique [57,58]. Modifications and extra assumptions related to the basic theory can be made to accommodate the specific arrangement and construction materials of the probe [59]. For easy measurement, the surface probe is usually insulated on one face so that heat only propagates towards the face of a flat specimen. The measurement accuracy depends on the specific probe and manufacturer and can be from 2 to 15% [44,45,60]. Figure 5 shows various types of surface probes.

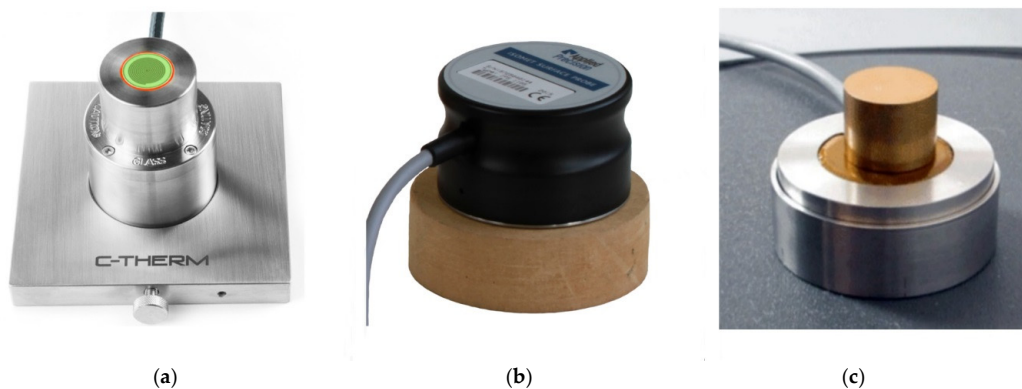


**Figure 5.** Various types of surface transient probes. The specimen or probe is large enough to ensure good contact. (a) Modified Transient Plane Source (MTPS) Sensor for TCi Thermal Conductivity Analyser [61]; (b) Surface probe for Isomet portable heat transfer analyser [45]; (c) Sensor for Hot Disk TPS Thermal Conductivity Instrument [60].

There also exist surface attachments that utilize needle probes and can be used in a similar way as the abovementioned sensors on the top of a flat and smooth sample. For example, Reference [44] uses a disk-shaped probe with a needle embedded in the underside of its body. Part of the heat generated by the needle penetrates into the sample material and part into the disk-shaped probe material (Figure 6). A correction method developed by Reference [44] uses the thermal parameters of the probe and sample to automatically determine the effective amount of heat entering into the sample material and evaluate the thermal properties of the sample. Examples of applications in soils/rocks can be found in References [62–65].

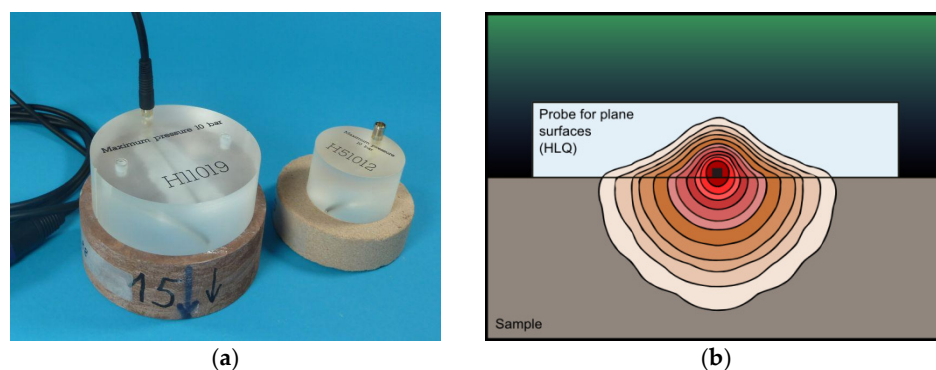


**Figure 6.** TeKa disk-shaped probe [44]. (a) TeKa disk-shaped material with embedded needle probe in the underside; (b) Heat profile in the disk-shaped material and sample, around the needle probe.

### 3.2.3. Optical Scanning Technique

The optical laser scanning technique is a noncontact optical method able to rapidly obtain a large number of measurements. In principle, the temperature of a sample is measured before and

after the passage of a constant heat source near the sample. Once again Fourier's law gives the link between thermal conductivity  $\lambda$  and the source power  $Q$ , the maximum temperature increase  $\Delta T$  and the distance  $x$  between the source and the sensor [66]:

$$\lambda = \frac{Q}{2\pi x \Delta T} \quad (3)$$

In practice, two infrared temperature sensors and a heat source are passed in front of black coated samples at a constant distance and constant velocity. The velocity of the scanning is based on the layer thickness required for the study, and is in the range of  $1\text{--}10 \text{ mm}\cdot\text{s}^{-1}$ . Measurement can be carried out either for plane or cylindrical surfaces of dry or saturated samples. The measurement may be performed directly on the rough surface (surface roughness of up to  $1.0 \text{ mm}$ ) covered with an optical coating ( $25\text{--}40 \text{ }\mu\text{m}$  thick) to minimize the influence of the varying optical reflection coefficient.

Reference standards with known conductivities  $\lambda_R$  are interspersed with samples and aligned along the scanning direction. The relation between the two thermal conductivities is given by:

$$\lambda = \lambda_R \frac{T_R}{T} \quad (4)$$

where  $T$  and  $T_R$  are the respective temperatures. The infrared radiometer continuously registers the temperature along the heating line, and a continuous thermal profile is provided. Measurements at various angles ( $\alpha$ ,  $\beta$ , and  $\gamma$ —see Figure 7) allow the determination of the thermal conductivity of anisotropic solids. The measurable range of thermal conductivity is  $0.2\text{--}70 \text{ W}\cdot\text{m}^{-1}\cdot\text{K}^{-1}$ , with a measurement error of around 3%.

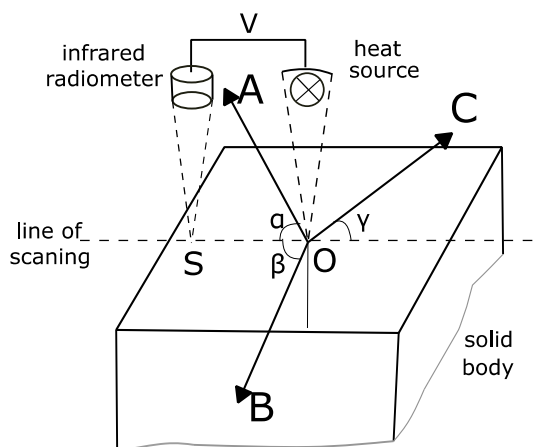


**Figure 7.** Principle of optical scanning method [66]. V: velocity of scanning; O: area of the heat spot; S: detection area of the radiometer; A, B, C: main axes of thermal conductivity with angles  $\alpha$ ,  $\beta$ ,  $\gamma$  to the line of scanning, respectively.

This technique has been used for measuring rock specimens. Reference [66] studied samples from 3 to 17 cm in length, 3–9 cm in width, and 2–6 cm in thickness. The technique can also be applied to rock core, as for example in Reference [67], where sandstone cores of 0.076 m in diameter and 0.5 m in length were studied. Thermal conductivity of 745-mm core samples from the Tarim basin in China was also determined using this technique [68].

### 3.3. Comparison of Methods

The measurement of thermal properties of soils and rocks has been tackled by different techniques in the literature, namely the guarded hot plate, the thermal cell, the divided bar, the thermal needle probe, the dual thermal needle probe, the transient plane source, and the optical scanning techniques.



These techniques allow the analysis of soil and rock samples in the centimetre to decimetre scale. However, not all techniques are suitable to all types of soils and rocks. This is because the nature of the specimens varies: cohesive and non-cohesive soils, rocks, different levels of water content and compaction levels, etc.

Direct comparison between the various available methods is hard to achieve as it would require studying samples under similar circumstances (collected in the same place, with the same water content and density conditions). As a result, the number of such comparisons in the literature is very limited, with those available being reviewed below. Figure 8 provides a comparison of measurements performed with transient and steady-state methods for a variety of soils at different saturation degrees and temperatures.

When testing relatively homogenous materials, both steady-state and transient methods are expected to give the same results. However, when dealing with heterogeneous materials, which is quite common for rocks or soils, one should expect that steady-state methods return more accurate and reliable values, provided that the sample size is large enough, heat losses are minimised, and no processes other than diffusion are occurring within the sample. Steady-state methods are claimed to be more accurate than transient methods, but there is actually little evidence to support that claim when it comes to soil analysis. In fact, Mitchel and Kao [69] reported that after evaluating several methods, the thermal needle probe was more appropriate due to its relative simplicity and rapid measurement time. Figure 8, however, shows that there is no trend between steady-state and transient test results taken across those available sources. However, there is a trend to utilise steady-state methods for rocks (solid mineral matter) and transient methods for soils (e.g., see Reference [40]).

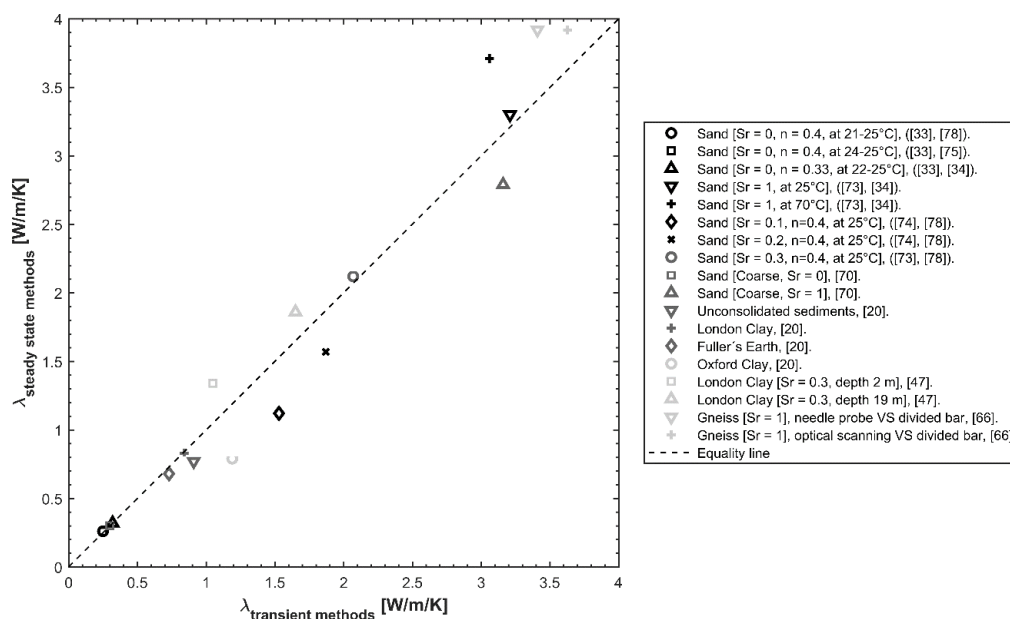


**Figure 8.** Comparison of transient and steady-state derived thermal conductivity ( $\lambda$ ) values based on data in References [20,33,34,47,66,70–74];  $S_r$ : degree of saturation,  $n$ : porosity.

In general, transient techniques can be applied to any type of soil under any water content condition [33], although it is important to make sure the size of any heating needles used are appropriate for the soil grain size. Jackson and Taylor [75], upon assessing transient methods, concluded that their main advantages are: (i) moisture migration in response to temperature gradients was minimised, and (ii) a long wait for thermal gradients to equilibrate was not required.

In an effort to quantify measurement uncertainties, Reference [20] reported higher thermal conductivity measurements obtained with the thermal needle probe (up to 10–20%) compared to the divided bar in unconsolidated sediments. This was in agreement with some studies, such as

Reference [19], but contradicted others, such as Reference [76], showing a general disharmony. The thermal needle probe did provide a lower thermal conductivity anisotropy in samples where measurements were performed in two perpendicular directions, as a result of the way that the heat was transferred by transient and steady-state methods.

Tarnawski and collaborators [33,71,72], who used the thermal needle probe, and Nikolaev et al. [34], who employed the guarded hot plate, constitute the most recent and complete studies on the dependency of the thermal conductivity of standard sands at different degrees of saturation over a temperature range. For dry sands, in Reference [34] agreement was demonstrated, with a maximum discrepancy of 5.7%, between the measurements performed with the guarded hot plate and the thermal needle probe, as reported by References [33,73,77,78] (see Figure 8). In saturated conditions, the guarded hot plate apparatus measured a maximum discrepancy of 5.2% lower than the reference data by Reference [78] at 25 °C. The variations do not seem significant, falling within the expected uncertainties of the methods. However, when in Reference [34] guarded hot plate and thermal needle probe measurements were compared for a range of temperatures from 25 °C to 70 °C, the steady-state method provided higher thermal conductivities than the ones reported by References [33,71]: 2.7%, 10%, and 17.5% at 25 °C, 50 °C, and 70 °C, respectively. This misfit is attributed to the water movement driven by a temperature gradient, i.e., buoyancy-driven water flow. Because of the short duration of the measurement with the transient method, this is practically non-existent. The phenomenon was also demonstrated by a finite element model.

Regarding unsaturated sands, Reference [72] claimed that the thermal needle probe data exhibit higher values than those obtained from guarded hot plate experiments (data from References [73,74] at 25 °C). They explained this on grounds of induced soil moisture redistribution by substantial temperature gradients applied to the tested samples during long-lasting guarded hot plate experiments, which leads to sample inhomogeneity. This behaviour has been identified at low degrees of saturations ( $S_r < 0.25$ ), yet there is not a clear trend for higher saturation degrees (see Figure 8).

The thermal cell method allows one to measure undisturbed clay samples and, in general, any kind of soil. However, reported comparative studies show that the thermal cell measurements overestimate the thermal needle probe estimations, with a difference up to 50% [47]. This disparity is mainly due to uncontrolled heat losses.

Popov et al. [66] compared the thermal needle probe, the divided bar, and the optical scanning techniques for the measurement of core rock samples. They obtained consistent measurements, as the deviation of the results from the three methods was less than 4%. However, they reported a higher scatter of the thermal needle probe technique as a consequence of point temperature measurements. They recommend the optical scanning technique when further information on thermal inhomogeneity and the three-dimensional anisotropy of rocks is required, as in References [67,79]. They recommend the divided bar method to characterize direction-dependent thermal conductivity.

Bilskie [50] validated the dual needle probe method for measuring soil (sand and loam) samples against estimations obtained from empirical models by Reference [16] for saturated sands. Smits et al. [80] also validated their dual needle probe setup against empirically predicted values by References [81–83]. This method is very sensitive to distance uncertainty and time resolution of the measured temperatures. Consequently, there is a risk that the distance between the needles may change if inserted into a hard soil.

There are no comprehensive comparative studies regarding the application of the transient plane source techniques in soils. However, their flexibility and the available sizes of sensors make them applicable to any kind of rock and soil [84].

Summing up, while measurements from transient and steady-state methods agree for dry soils (or those with low moisture content), there is no agreement for soils with high moisture contents and temperatures above 50 °C (see Figure 8). The current status still resembles that described by Reference [20]. As specimens are prepared in different ways, any comparison between methods can only be limited. It is hard to reproduce thermal properties values in different laboratories, especially

for clay and mudstone samples, and when employing surface probes on soils and rocks. There is a lack of standardised procedures focused on soil thermal property lab testing that guide the sampling, specimen preparation (compacting and saturation processes), and measuring processes. Therefore, it is essential to understand the advantages and limitations of each method before its use. A summary of the advantages and limitations of each technique used for measuring soil and rock thermal properties is provided in Table A1 in the Appendix A.

#### 4. In Situ Thermal Testing (Thermal Response Tests)

Thermal response testing (TRT) is a widely used in situ method for the characterisation of ground thermal properties for shallow geothermal energy applications, in particular for borehole and pile heat exchangers. The most common application of thermal response testing involves the measurement of undisturbed ground temperature, ground thermal conductivity, and thermal resistance of the ground heat exchanger [85,86], which are critical design parameters for the design and analysis of borehole and pile heat exchangers. Undisturbed ground temperature is a key thermo-geological parameter needed for the assessment of the geothermal potential of an area. The temperature difference between the undisturbed ground temperature and the mean heat carrier fluid temperature circulating in the heat exchanger leads directly to the heat transfer between the ground heat exchanger and the surrounding ground. Ground with higher thermal conductivity not only yields larger heat transfer rates but also recuperates more rapidly from thermal depletions and thermal build-ups. Thermal resistance of the ground heat exchanger,  $R_b$  ( $\text{m}\cdot\text{K}\cdot\text{W}^{-1}$ ), is the effective thermal resistance between the heat carrier fluid in the ground heat exchanger and the surrounding ground. A lower value of thermal resistance leads to better system performance, a smaller ground heat exchanger size, and a lower installation cost.

A thermal response test is usually performed to assist the sizing of ground heat exchanger fields. Its execution is recommended for installation capacities larger than 30 kW [87]. This section complements earlier reviews on the topic [88–91], and presents the state of the practices and methodologies adopted in thermal response testing. In the following sections, the basic constructs of thermal response testing are described, introducing undisturbed ground temperature estimations techniques, standard testing procedures, and main analysis methods. This provides the basis for more innovative thermal response test practices such as distributed and enhanced thermal response tests and the thermal response testing of pile heat exchangers.

##### 4.1. Undisturbed Ground Temperature

For SGE applications, the ground temperature is characterised by three different ground zones: surface, shallow, and relatively-deep. Temperature profiles of the surface ground zone (i.e., top few centimetres) and the shallow ground zone (i.e., from the surface zone to a few meters down) vary with the diurnal and seasonal changes of ambient air temperature, respectively. Underground temperature of the relatively-deep zone (i.e., from the shallow zone to few hundred meters down) increases slowly with depth due to the geothermal gradient.

In most practical cases, especially concerning vertical borehole applications, a single value of average ground temperature, generally referred to as the undisturbed ground temperature, is used as a design parameter. Several studies, including References [92–98], have underlined the significance of undisturbed ground temperature, and have shown its effect on factors including sizing of the ground heat exchanger, extracted thermal power, and performance of the heat pump, among others.

The undisturbed ground temperature is determined, in situ, by mainly two methods, i.e., downhole temperature logging, and the fluid circulation method [88]. In the downhole temperature logging method, the temperature distribution along the borehole depth is measured by means of a downhole temperature sensing system. A simple or weighted average of the measured temperature values is then used to approximate the undisturbed ground temperature. Various downhole temperature measurements systems, including wired temperature sensors, submersible wireless probes, and fiber optics, among others, are used in practice. This method is relatively easy to apply to groundwater-filled

boreholes, where the temperature measurements can generally be taken by lowering the downhole sensors in the spacing between the heat exchanger pipes and the borehole outer wall. The downhole sensing system is generally retracted after performing the measurements. In grouted boreholes, the application of downhole temperature logging is slightly more complicated. Measurements in the spacing between the heat exchanger pipes and the borehole wall can only be taken if a permanent downhole temperature sensing system has been installed before grouting the borehole. Otherwise, the temperature can only be measured inside the heat exchanger pipes. It is important that the heat carrier fluid is kept in the pipes long enough to reach thermal equilibrium with the surrounding ground. It is also important to submerge the sensing element slowly to prevent any disturbance of the fluid in the pipes.

The fluid circulation method involves circulating the heat carrier fluid through the undisturbed borehole without injecting or extracting any heat. Firstly, the fluid is kept long enough in the heat exchanger pipes to reach equilibrium with the surrounding ground. Then, the undisturbed ground temperature is estimated from the fluid temperature exiting the ground heat exchanger. The most common approach is to circulate the fluid in the ground heat exchanger until temperature variations peter out, and the circulating fluid temperature stabilises. The stabilised fluid temperature is then taken as an approximation of the undisturbed ground temperature. A second approach [99] is to use the minimum temperature value of the heat carrier fluid exiting the ground heat exchanger during the first circulation cycle as an estimation of the undisturbed ground temperature. A third approach is to take the average temperature of the fluid exiting the ground heat exchanger during the first circulation cycle as an estimate of the undisturbed ground temperature.

When using the fluid circulation measurement method, several factors, including fluid temperature outside the ground loop, heat gains from the circulation pump, ambient coupling, and fluid residence time in the heat exchanger, may affect the undisturbed ground temperature measurements. This is particularly relevant if the fluid is circulated through the ground heat exchanger more than one time. Javed and Fahlén [100] and Gehlin and Nordell [101] compared various approaches to measure undisturbed ground temperatures on a multi-borehole field and a single borehole, respectively. The results of both these studies suggest that the average temperature of the fluid exiting the ground heat exchanger during the first circulation cycle provides the best estimate of the undisturbed ground temperature. On the contrary, the stabilised fluid temperature and the minimum fluid temperature approaches are both shown to have serious shortcomings. The undisturbed ground temperature value could be greatly influenced by ambient coupling and heat gains from the circulation pump when using the stabilised fluid temperature approach. Similarly, the minimum recorded temperature approach could result in strongly underestimated undisturbed ground temperature value, especially with low ambient temperatures during the measurement.

When measuring the undisturbed ground temperature, it is necessary to pay attention to the effects of urbanisation and other anthropogenic activities on the measured temperature values [102–107]. Elevated ground temperatures and zero or negative ground temperature gradients should be expected and allowed in the design of shallow geothermal systems in close proximity to existing facilities including buildings and structures, or in urban areas.

#### 4.2. Thermal Response Testing

A thermal response test consists of measuring the temperature evolution of a ground heat exchanger under a prescribed thermal load. Several variations of the test procedure exist e.g., References [86,108–113].

The thermal response test variants differ based upon their operation mode (i.e., heating or cooling), boundary conditions (constant heat flux or constant input temperature), analysis period (active phase or recovery phase), and measurement system (standard, distributed, or enhanced sensing), among others. However, the common principle upon which all variants of thermal response tests are

based is capturing the thermal response of the ground to a known thermal excitation, and evaluating ground and borehole thermal properties using a suitable heat transfer model.

Despite all its variants and recent developments, the conventional approach to thermal response testing remains the most prevalent and universal approach, and is the preferred testing method for estimating ground and borehole thermal properties. This is due to the simplicity of design, implementation, control, and evaluation of the conventional approach. When performed in the conventional way, the standard methodology of thermal response testing begins with measuring undisturbed ground temperature, followed by constant power heat injection or extraction for a period of 2–3 days. Most often the testing is performed in heat injection mode to minimise the influence of external factors affecting the measurements. An electric resistance heater is typically used to heat the heat carrier fluid at a constant power rate  $q$  of  $50\text{--}80\text{ W}\cdot\text{m}^{-1}$ . The temperature of the heat carrier fluid entering and leaving the borehole is measured, together with the flow rate, ambient temperature, and input power to the electric heater and the circulation pump. Measurements are taken at regular intervals of 1–10 min. Finally, measurements are analysed using a mathematical heat transfer model, most commonly the infinite line source approximation, to evaluate ground thermal conductivity and borehole thermal resistance values. Figures 9 and 10, respectively, show schematic diagrams of a typical thermal response test setup, and the most typical measurements taken during a standard thermal response test.

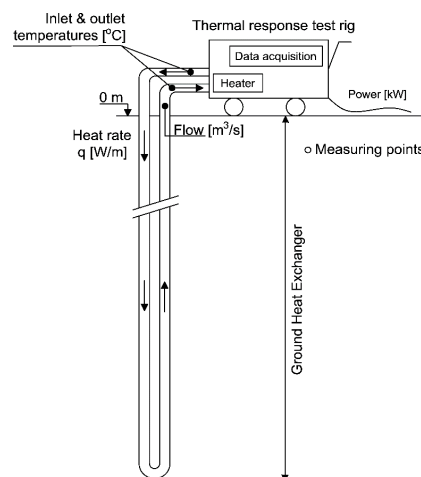


Figure 9. Thermal response test setup, after Reference [86].

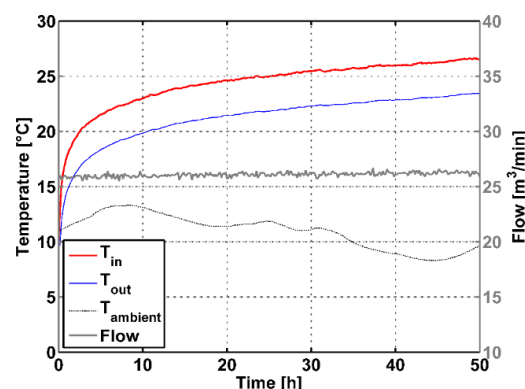


Figure 10. Thermal response testing (TRT) field data of a 100m-deep single U borehole heat exchanger (VIA 14), collected in Denmark [114].

Evaluation of thermal response tests can be carried out using direct or parameter estimation methods. Direct evaluation methods are based on simplified approximations of infinite line source [115] and infinite cylindrical-source [116] solutions. To use the direct methods, thermal power injected to the borehole or extracted from it should remain almost constant over the whole test duration. The standard deviation of the input power should be less than  $\pm 1.5\%$  of the mean input power, and the maximum variation should be smaller than  $\pm 10\%$  [117].

Of the direct methods, the infinite line source approximation method is easiest to implement and is widely used because of its simplicity and strong intuitive appeal. The method involves plotting experimentally measured mean temperatures of heat carrier fluid entering and exiting the borehole heat exchanger against logarithmic time, and using a straight line to fit the experimental measurements. The line source approximation is mostly recommended for times larger than  $20 r_b^2/\alpha$ , which generally accounts to 10–20 h for a typical borehole. This is due to the limitation of the infinite line source approximation to match the original model at smaller times—the error of the approximation for time  $5 r_b^2/\alpha$  is 10% and for time  $20 r_b^2/\alpha$  is less than 2.5%. The slope and intercept of the straight line are used to calculate ground thermal conductivity [86] and borehole thermal resistance [118], respectively.

Parameter estimation methods allow the analysis of thermal response tests with power variations higher than those deemed acceptable with direct evaluation methods. Parameter estimation methods account for variations in input power by considering stepwise-constant heat pulses rather than an overall constant input power. These methods initially use estimated values of ground conductivity and borehole resistance to simulate the heat carrier fluid temperature. The estimated values are then optimised by minimising the error between simulated and experimentally measured fluid temperatures. Parameter estimation methods for evaluating thermal response tests are based on both analytical as well as numerical models. Several parameter estimation methods have been implemented in high-level programming languages and are available as standalone computer programs. These include, among others, Geothermal Properties Measurement (GPM) [119], Vertical Borehole Analysis and Parameter Estimation Program [120], and TRT Evaluation Program (TEP) [121]. Software tools GPM and Vertical Borehole Analysis and Parameter Estimation Program are, respectively, based on one-dimensional finite-difference and two-dimensional finite-volume models, whereas software tool TEP is based on the analytical method proposed by Reference [122]. Parameter estimation methods based on infinite line source and infinite cylindrical-source approximations have also been implemented by individual users in spreadsheets and mathematical analysis software [94].

One important factor when analysing thermal response tests is that there could exist more than one combination of the ground thermal conductivity and borehole thermal resistance values that can match the experimentally measured temperature curve [123]. However, as noted by Reference [124], the two parameters have counterbalancing effects on the design, and using the experimentally determined values of both parameters mitigates some of the error that would occur if only the ground conductivity value estimated from the test is used for the design. It is still, however, recommended to separately calculate the borehole thermal resistance value to counter-check the experimentally determined value. Several methods to calculate borehole thermal resistance have been presented and compared in References [125,126]. A lower value of borehole thermal resistance improves the performance of the system and lowers the total required borehole length. A key factor in this regard is the choice of the grouting material between heat exchanger pipes and the surrounding ground [8,127].

Thermal response tests are subjected to possible errors caused by uncertainties in measurements, in (input) design parameters, and in the analysis method. Uncertainties in measurements arise from factors such as imprecise location, calibration, or limitations of the measuring instruments and fluctuations in the test environment. Air trapped in the pipes can also cause severe measurement inaccuracies concerning water flow rate and can negatively affect the heat transfer to the ground. Uncertainties in design parameters are caused by inaccessible, incomplete, or inaccurate data on material properties (e.g., densities and heat capacities of heat carrier fluid), geometrical dimensions (e.g., diameter and depth of borehole), and boundary and input conditions (e.g., undisturbed ground



temperature). Uncertainties in the analysis method are attributable to the inherent limitations of mathematical models used to determine ground conductivity and borehole resistance values as well as the duration of thermal response tests. In References [100,120,128], detailed uncertainty analyses of thermal response tests were presented. The overall uncertainty for each of these studies, when determined by adding all of the individual uncertainties in quadrature, are approximately  $\pm 5\text{--}10\%$  for ground thermal conductivity and  $\pm 10\text{--}15\%$  for borehole thermal resistance. Taking a somewhat different approach, Javed [129] evaluated nine boreholes in close proximity using the commonly-used infinite line source approximation method, and found overall experimental uncertainties of  $\pm 7\%$  in ground conductivity value and  $20\%$  in borehole thermal resistance value.

Thermal response test results have been shown to be highly sensitive to several factors, which include climatic conditions, groundwater flow, input power variations, test duration, and analysis method. Climatic conditions cause undesired heat exchange to or from the thermal response test setup. It has been demonstrated that ground conductivity estimations inferred from thermal response testing can be affected by a factor of one third if energy losses outside the borehole are neglected [130]. Figure 11 shows an example of a thermal response test that has been strongly affected by ambient weather conditions. When performing a thermal response test, pipe connections between the test rig and the borehole, and other components of test rig including accumulator tank, circulation pump, etc., must be thermally insulated to prevent, as far as possible, the transfer of heat between the heat carrier fluid and the ambient air. A few methods to assess and eliminate the effects of ambient conditions on thermal response tests are also available [99,130].

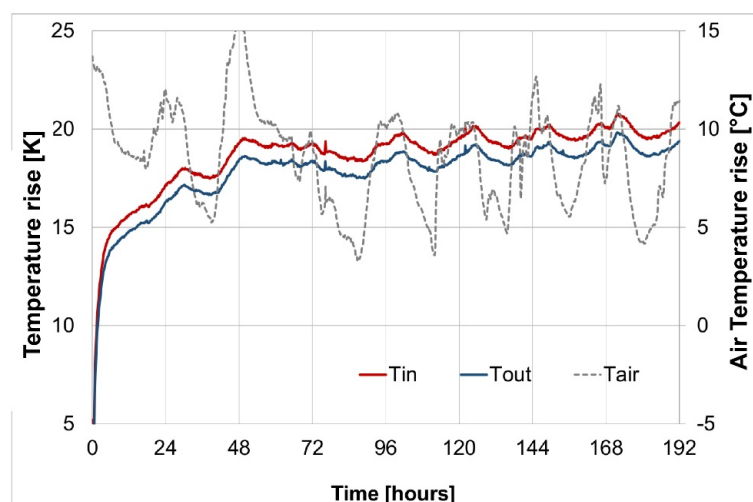
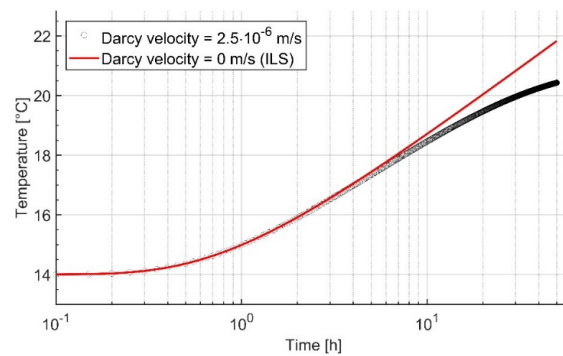


Figure 11. Example of a thermal response test affected by ambient conditions.

Thermal response test measurements may also be affected by hydrogeological conditions. In the presence of significant groundwater flow, ground thermal properties evaluated by the commonly-used infinite line source approximation are invalidated. Figure 12 shows the evolution of heat carrier fluid temperatures, simulated for two cases, one with and one without groundwater flow. It can be clearly observed that due to the enhanced heat transfer between the heat carrier fluid and the ground, the evolution of heat carrier fluid temperature over time is inhibited by the presence of groundwater flow. When evaluating a test with significant groundwater flow, the enhanced heat transfer translates into a higher but inaccurate estimation of ground thermal conductivity, which continuously increases with the analysis time. It is recommended to always perform a sequential analysis [131] when evaluating a thermal response test to explore the effect of groundwater flow on the test results. Groundwater flow-influenced thermal response tests can alternatively be evaluated using a moving line source or other advection-based analytical or numerical methods, including those suggested by References [132–135].



**Figure 12.** Evolution of borehole heat exchanger fluid temperatures in a heating process, considering groundwater flow against the conduction-based infinite line source [132].

The accuracy of thermal response test results also depends on power variations during the test. Direct evaluation methods, including the infinite line source approximation, assume constant heat injection or extraction rates. When these methods are used for the evaluation of thermal response tests, fluctuations in supply power can lead to inaccurate results. In case of significant power variations, either effects of variable heat rates should be removed from the test [136], or parameter estimation methods should be used for evaluating the tests [94,137,138].

The duration of a thermal response test greatly influences the accuracy of the estimated results. A longer test duration yields more accurate and reliable evaluation of ground and borehole thermal properties. This is because longer test durations allow borehole heat transfer to reach quasi-steady state, while simultaneously reducing statistical errors due to power and thermal fluctuations. The American Society of Heating, Refrigerating and Air-Conditioning Engineers [117] h. However, in References [139,140], minimum test durations of 50 and 60 h were emphasised, respectively. Long-duration thermal response tests (>100 h) were performed in References [120,129] to study the effects of different test lengths on the estimated properties. Their findings suggest that ground conductivity and borehole resistance estimates converge for test durations longer than 100 h. For test durations between 50 and 100 h, the estimated results have a maximum absolute deviation of approximately 5% of the converged values. For test durations shorter than 50 h, the errors in estimated ground conductivity and borehole resistance values are much larger. In Reference [118], a method to calculate the minimum test duration necessary to estimate ground thermal conductivity within 10% of the converged value from a long TRT was developed.

#### 4.3. Distributed and Enhanced Thermal Response Testing

Conventional thermal response tests give average values of ground conductivity over the entire length of the borehole heat exchanger. It is not possible to measure thermal conductivity for different geological layers with a conventional test. Identifying vertical contrasts in thermal conductivity along the borehole depth may allow for the optimisation of borehole designs with respect to their placement, size, and depth.

Distributed and Enhanced Thermal Response Tests (DTRTs and ETRTs) are testing methods that measure variations in ground thermal conductivity along the entire length of the borehole heat exchangers. Both methods rely on temperature measurements taken at multiple depths along the borehole, using downhole sensors placed in the grout, or inside or outside the ground heat exchanger pipes. A distributed thermal response test [107,141–145] is very similar to a standard thermal response test. It consists in injecting heat to, or extracting heat from, the borehole heat exchanger at constant power and measuring thermal response of the ground at multiple instances along the borehole depth. The measurements are obtained by means of temperature sensors (e.g., thermocouples, thermistors, resistance temperature detectors) or fiber optic cables. Figure 13 shows examples of downhole

installation of temperature sensing and fiber optic elements used for distributed thermal response testing in practice.

An enhanced thermal response test [113,146] involves injecting heat into the ground by means of one or more copper heating cables and measuring the vertical ground temperature distribution with an optical fiber cable. Generally, the copper and optical fiber cables are integrated in one single ‘hybrid cable’. The hybrid cable is shaped and sized after the ground heat exchanger, and is placed on the outside of the heat exchanger. Figure 14 shows component and installation details of hybrid cables used for enhanced thermal response testing.

The main reason for using fiber optics for distributed and enhanced thermal response testing is the acquisition of a high-resolution temperature distribution along the borehole depth. Each fiber is connected to a Distributed Temperature Sensing (DTS) equipment, which injects laser light. The signal is scattered and reemitted from the observed point. The backscattered signal consists of light scattered by a variety of mechanisms. Among these, the anti-Stokes Raman backscatter signal is sensitive to temperature and is used to measure the temperature profile along the fiber length. The position of the temperature reading is determined by the arrival time of the reemitted light pulse. The use of DTS in thermal response testing allows measurements of high spatial, temporal, and temperature resolution. Tests with spatial resolution of 0.2–5 m, temporal resolution of 1–10 min, and temperature resolution of 0.1–0.5 K are considered state-of-the-art today.

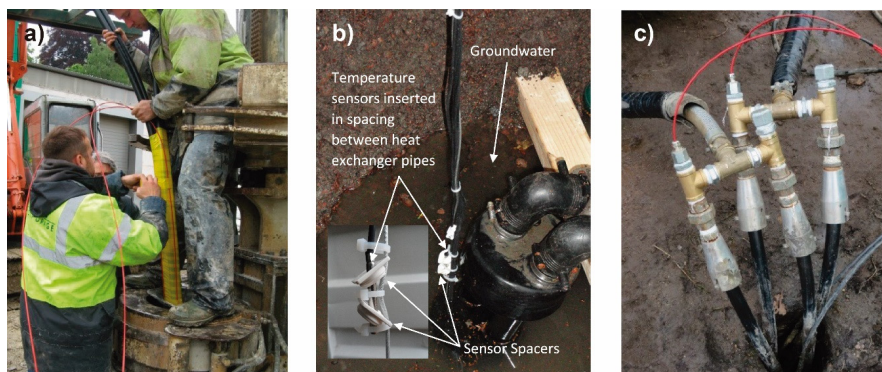


**Figure 13.** Construction details for distributed thermal response tests (a,b) Installation of temperature sensors at the outer surface of U-pipes; (c) Fiber optic cables fitted inside the heat exchangers after borehole execution (Limelette, Belgium).

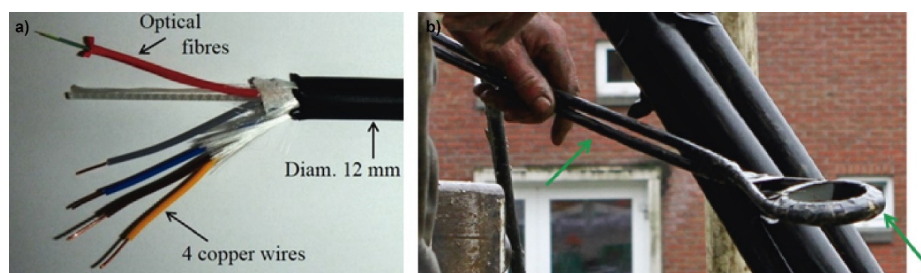


**Figure 14.** Hybrid cables for enhanced thermal response testing (a) Picture of a hybrid cable with indication of all different components; (b) U-loop of the hybrid cable, to be attached to the bottom of the borehole heat exchanger before their installation in the borehole.

The analysis of distributed and enhanced thermal response tests is also quite similar to that of a conventional thermal response test, but with a few modifications. When analysing a distributed or an enhanced thermal response test, the borehole is divided into several smaller zones, each of 0.5 m or larger. For each zone, mean fluid temperature and difference between inlet and outlet

temperature values are obtained from the vertical temperature measurements taken along the borehole (see Figure 15). Thermal power to each zone is determined as a multiple of the mass flowrate of the heat carrier fluid times the difference between zone inlet and outlet temperatures. For an enhanced thermal response test, the injected power is constant for the entire borehole length and can be directly calculated from the electric power supplied to the heating cable. The analysis is performed separately for each zone, and corresponding estimations of thermal conductivity and borehole resistance are obtained. The analysis can be performed using any of the evaluation methods described earlier, though infinite line source approximation is mostly used. For better accuracy, it is common to carry out the analysis in the recovery phase, especially for enhanced thermal response tests.

Several recent studies have demonstrated the advantages of distributed and enhanced thermal response tests over conventional tests. These tests have been successfully used to identify and characterise hydraulic fractures (e.g., [144,147]) and ground layers (e.g., [141–143]). An example is also presented here to demonstrate the advantages of a distributed temperature sensing-based thermal response test over a conventional test. Figure 16 shows the thermal characterisation of the subsurface based on two nearby boreholes in Limelette, Belgium. The boreholes are 74 and 120 m deep, and are separated by about 6 m. Conventional and enhanced thermal response tests were carried out on both boreholes. The test parameters and results are summarised in Table 1. The ground conductivity estimations obtained from the conventional thermal response test and the average values obtained from the enhanced thermal response tests are very similar. There is a maximum difference of about  $0.3 \text{ W} \cdot \text{m}^{-1} \cdot \text{K}^{-1}$  in the ground conductivity estimations from the two methods. However, as demonstrated in Figure 16, the enhanced thermal response test provides comprehensive breakdown of thermal conductivity values along the borehole.

In Figure 17, average ground thermal conductivity estimates from distributed and enhanced thermal response tests are compared to conventional test-based estimates, as reported in the literature. In all cases, results from the distributed and enhanced tests are in quite good agreement with the corresponding TRT estimates, with differences less than 10%. The results of the enhanced thermal response tests presented in this paper also displayed a similar tendency, as shown in Table 1.

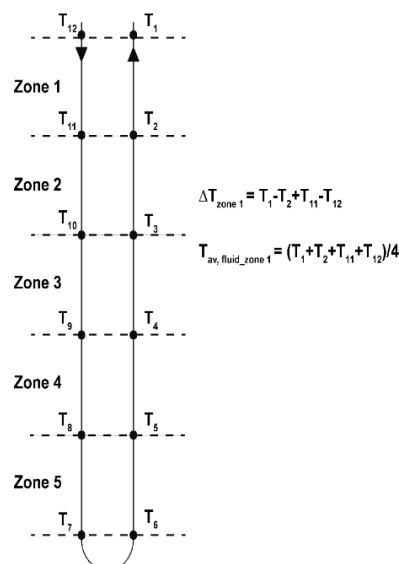


**Figure 15.** Schematic illustration with regard to the analysis of distributed and enhanced thermal response tests.

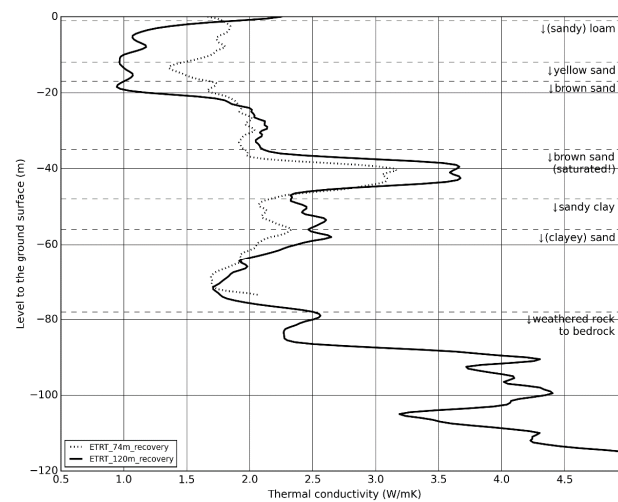


**Figure 16.** Comparison of the thermal conductivity resulting from enhanced TRTs for a 74-m-deep and a 120-m-deep borehole in Limelette (Belgium), separated by about 6 m. Based on data from the Smart Geotherm project funded by the agency Flanders Innovation and Entrepreneurship.

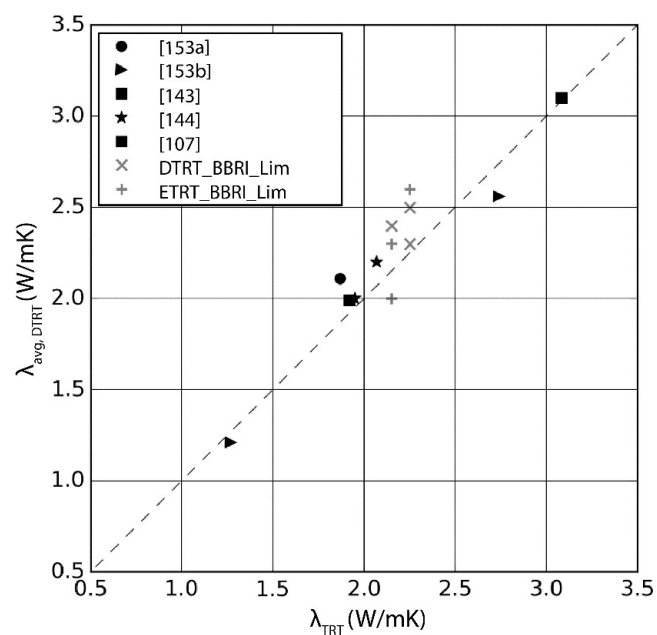


**Figure 17.** Average ground thermal conductivity by distributed thermal response tests (DTRTs), enhanced thermal response tests (ETRTs), and conventional TRT values as reported in References [107,143,144,148].

**Table 1.** Comparison of the classical and enhanced thermal response tests on two nearby boreholes in Limelette (Belgium).

| Parameter                    | Borehole 74-m-Deep                         |  | Borehole 120-m-Deep                        |  |
|------------------------------|--|--|--|--|
|                              | Standard TRT                               | Enhanced TRT                           | Standard TRT                               | Enhanced TRT                           |
| Injected power               | 53 W/m                                     | 28 W/m                                 | 56 W/m                                     | 23.1 W/m                               |
| Flow rate                    | 0.26 l/s                                   | -                                      | 0.25 l/s                                   | -                                      |
| Heating phase duration       | 136 h                                      | 84 h                                   | 117 h                                      | 96 h                                   |
| Recovery phase duration      | -  | 60 h                                   | -  | 124 h                                  |
| Average thermal conductivity | 2.1–2.2 W·m <sup>-1</sup> ·K <sup>-1</sup> | 2.0 W·m <sup>-1</sup> ·K <sup>-1</sup> | 2.2–2.3 W·m <sup>-1</sup> ·K <sup>-1</sup> | 2.6 W·m <sup>-1</sup> ·K <sup>-1</sup> |

Based on data from the Smart Geotherm project funded by the agency Flanders Innovation and Entrepreneurship.



There are also considerations and constraints when using distributed and enhanced thermal response tests. One significant aspect that needs to be considered when using distributed temperature sensing is that, unlike other temperature sensors, fiber optic measurements require continuous in situ calibration. This is because any change in the operating conditions of the optical fiber and the DTS equipment (e.g., ambient temperature), alters the calibration parameters [145,149]. It is, hence, necessary to place a section of the optical fiber into a known-temperature environment, e.g., water or ice bath, during the whole testing procedure for offset calibration. Moreover, longer fiber lengths also need to be adjusted for slope losses, thus requiring calibration measurements at two different sections of the fiber optic. Furthermore, when evaluating distributed or enhanced thermal response tests, it is often assumed that there is no heat transfer between different zones, like those shown in Figure 15. However, this assumption is void if different geological layers with significantly different ground thermal conductivities are present, which can significantly affect the test results [150]. Also, the distributed temperature measurements depend on the location of the fiber in the heat exchanger, and the relative position of the heat exchanger pipes to each other. As these positions are unknown, and may also vary along the borehole depth, there are certain intrinsic errors in calculating the average fluid temperature for each zone. Due to these and other potential problems and limitations in applying distributed and enhanced thermal response tests, there exist certain uncertainties in ground properties estimated from these approaches, an example of which can also be seen in Figure 16 for two enhanced thermal response tests performed on two nearby boreholes.

#### 4.4. Thermal Response Testing of Foundation Pile Heat Exchangers

Energy piles are energy geostructures that utilise reinforced concrete foundation piles as heat exchangers. Pile heat exchangers are less slender than borehole heat exchangers, being shorter and wider than the latter, hence yielding lower aspect ratios (length/diameter). Borehole heat exchanger aspect ratios range from 100 to 1500, whereas energy pile aspect ratios are typically smaller than 50. Energy piles consist of reinforced concrete (instead of grout) and their structural integrity is prioritised over thermal performance for obvious reasons. Energy piles vary in length, typically between 10 to 50 m with a diameter from 0.3 to 1.5 m, utilising different types of design geometries [151] (see Table A2 in the Appendix A).

However, due to the underlying similarities between the borehole and pile heat exchangers, attempts have been made to adapt the thermal response testing practice and interpretation methods to energy piles [152]. Longer duration thermal response tests are usually needed for pile heat exchangers due to their larger diameter—and, hence, thermal mass—in comparison to traditional borehole heat exchangers. The testing procedure remains similar to that for borehole testing. However, there is a lack of scientifically supported guidelines for the interpretation of energy pile thermal response test data. International guidelines limit the practicability of field testing energy piles to diameters up to 0.3 m because of time and cost restrictions [153]. Table A2 provides a summary of studies where strict use of the thermal response testing method has been adopted for pile heat exchangers to determine the soil thermal conductivity.

When analysing energy pile thermal response test data, models that have been developed for vertical borehole heat exchangers, such as the infinite line source [116], are generally applied. However, large diameter and short aspect ratio heat exchangers deviate from traditional, generally assumed line source behaviour. When using the line source model to evaluate thermal response tests, the thermal response after a few hours is assumed to be log-linear with respect to time. For low aspect ratio piles, this linear behaviour never truly occurs as three-dimensional effects (i.e., surface boundary conditions and end effects), causing the actual thermal response of piles to diverge from that of line source solutions [154]. The axial effects imply that the measured temperatures always fall below the line source modelled temperatures, which further implies that the line source-based interpretation will systematically overestimate the thermal conductivity.



In the dimensioning of borehole heat exchanger fields, the borehole thermal resistance is considered constant, as it is assumed that the borehole heat exchanger reaches a steady-state condition after a few hours of operation. However, piles can take days or even months to reach a steady-state condition and the assumption of constant pile thermal resistance neglects the thermal inertia related to large diameter piles [154].

To appropriately interpret thermal response test data from pile heat exchangers, a number of alternatives exist (Table A2), either in the form of analytical solutions, (semi)empirical functions, or 2- or 3D numerical models. The first category includes analytical solutions such as the line and cylindrical source finite solutions suggested by References [116] and [115], the finite line source solution presented by Reference [155], the composite cylindrical model to account for the contrasting thermal properties of the pile and the soil reported in References [156,157], the infinite solid cylindrical heat source model described in References [91,158], and semi analytical models such as those described in Reference [159]. The second category includes temperature response empirical functions (so-called G-functions), e.g., see Reference [154], which are developed for specific ranges of pile heat exchanger geometries and provide temperature solutions for different pile aspect ratios (shown in Figure 18). The final category potentially constitutes the most accurate means to back-analyse thermal response tests and estimate thermal parameters. However, the computational effort of a full 3D numerical model-based interpretation is potentially too burdensome for routine thermal design.

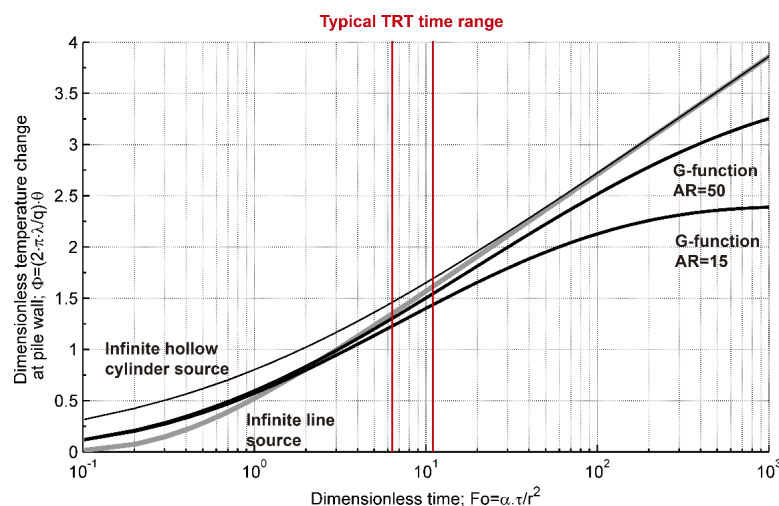


**Figure 18.** Line source solutions together with pile heat exchanger G-functions [154] for different aspect ratios (AR) and typical TRT time ranges.

Zarrella et al. [160] recently back-analysed a thermal response test on a 20-m-long, double U-tube 0.6m diameter energy pile near Venice (Italy). The geological setting includes alternating layers of clay and silty sand. The inversion of measured temperatures utilises a detailed numerical forward model based on an electrical analogy, making use of lumped thermal capacities and resistances [161]. Comparing this interpretation with the traditional line heat source approach, the authors found that the latter approach led to ground conductivity estimates roughly twice the numerical model-based estimate. This suggests that the choice of interpretation method can cause significant errors in the dimensioning of the overall system. Thus, the authors recommend the use of an interpretation method that accounts for 3D effects and the actual geometry of the pile. Similar conclusions are drawn in Reference [162], where synthetic data from a 3D finite element model of a 1m diameter pile was used to find an upper bound of 50% for the error in estimating thermal conductivity when using the line source model. In Reference [163], a 3D numerical finite element model was employed to simulate short-term TRTs on prototype 0.4 m diameter precast energy piles placed in partially saturated weathered granite

in Korea. Similar to the findings of Reference [162], the numerical assessment of thermal conductivity resulted in values of about half of those estimated by conventional 1D analysis.

An analogous fully 3D numerical approach was also employed in References [164,165], where the experimental results of a multi-stage, one-month-long TRT of a 0.3 m diameter test pile installed in London clay were reproduced. The same data were analysed in Reference [166]. Soil thermal conductivity was estimated with a numerical method, the infinite line source, and the pile G-functions proposed by Loveridge and Powrie (2013) [154]. The line source method overestimated the ground thermal conductivity values by up to 20% compared to the numerical method. The values estimated from empirical methods such as G-functions were closer to those from the 3D numerical model, with a maximum difference of 10%.

Based on the above studies and similar outcomes from other authors (e.g., [157,167,168]), it is demonstrated that the use of numerical methods to back-analyse TRT data on energy piles is a more accurate way to estimate soil and concrete thermal parameters. These methods are preferred over traditional 1D methods, especially when referring to short duration TRT data, and/or analysing large diameter, multiple U-tube, low conductivity concrete, or otherwise less conventional energy piles. One possible shortcoming of numerical methods is their computational expense, and the characterisation they require, which is generally greater than other methods and can make them unsuitable for routine practical usage. In this respect, the use of (semi)empirical methods such as G-functions can be an advantage, as they represent a compromise between reliability and ease of use/computation time.

## 5. Scale in Thermal Properties Measurement

This paper has so far considered the features of different methods of small-scale laboratory testing for thermal properties (Section 3), as well as the procedures for carrying out and interpreting large-scale in situ thermal response tests (Section 4). While work has been carried out on both these topics by a number of researchers, there remain fewer case studies where high-quality testing, both in situ and at the laboratory scale, has been carried out on the same materials from the same locations. This is an important area, since other diffusive properties of geological materials, e.g., hydraulic conductivity, are well known to be scale-dependent. This is especially true for heterogeneous media (e.g., [169]). There are also differences between the testing methods themselves that are applied at different scales which may affect the results. We show below from a literature review that the in situ values of thermal conductivity are significantly greater than laboratory-derived values and further discuss this systematic discrepancy using examples as appropriate. This is followed by a discussion of how we can upscale from field and laboratory analysis to regional scale assessments of properties or geothermal potential.

### 5.1. Comparison between Laboratory and Field Thermal Characterisation

Table A3 in the Appendix A reports known cases where in situ testing for thermal conductivity has been carried out on boreholes or piles when measurements have also been made in the laboratory. The results of these tests are then summarised in Figure 19 below. The results span deep boreholes, large-scale laboratory tests, and a variety of energy piles. Most of the laboratory testing were conducted with the needle probe, although there are also some cases of other transient methods. In situ measurements are all made with thermal response tests (TRT), the majority of which are interpreted using the line source approximation, although there are two cases of finite element analysis (FEA) being used.

It can be seen from Figure 19 that in most cases the field scale tests give rise to larger values of thermal conductivity, with a maximum factor of 2 in the reported studies, which is much greater than the observed inter-TRT variability (Figure 17). There are a number of reasons that could explain these results, which are discussed in the sections below.

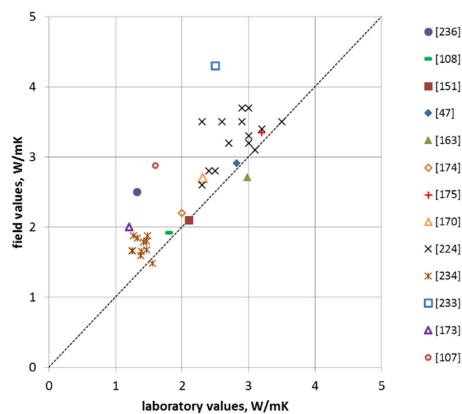


**Figure 19.** Comparison of laboratory and field-derived thermal conductivity values based on data in References [47,107,108,152,163,170–177].

#### 5.1.1. True Scale Effects

Laboratory tests, and especially transient tests with a short duration, will thermally activate a much smaller volume of soil or rock compared to borehole scale thermal response tests. Therefore, the presence of fabric, structure, or large-scale fracturing, which may be present at the metre scale in the field, will not be considered in laboratory tests, which typically have a representative elementary volume on the centimetre scale. Depending on the nature of these features and their orientation compared to the heat flow direction, they may lead to higher or lower thermal conductivity. Furthermore, recent studies have shown that even very small-scale heterogeneities can influence intermediate-scale thermal properties, with effective thermal conductivity of rock core determined to be less than the average of smaller scale point measurements [79].

#### 5.1.2. Groundwater Effects

One factor of scale which will always results in higher values of effective thermal conductivity is the presence of advecting groundwater (e.g., [140]) within pore spaces or especially fractures. It is interesting here to note the observations in Reference [170], where 57 boreholes were tested in situ and compared the results of laboratory tests on 1398 rock core samples. They found that those geological formations which were known to be karstic, highly fractured, or porous and were thus associated with regional flow conditions, were also the formations where there was the biggest difference between laboratory and field scale thermal conductivity values. This is consistent with groundwater movement being one of the major causes of laboratory/field discrepancies.

#### 5.1.3. Sampling Issues

It is almost impossible to take a truly undisturbed soil sample. For the granular soils in Figure 19, the laboratory tests were performed on reconstituted samples. These samples may have been prepared at voids ratio or moisture contents not entirely representative of field conditions. For clay soil, it is well known (e.g., [178]) that the shearing induced by the process of sampling will both locally change the structure of the clay and also effect its moisture content. Samples may also dry over time if not well sealed or tested rapidly (e.g., as is the case in Reference [47]). The latter factors in particular could lead to a systematic underestimation of thermal conductivity from laboratory tests, since the results are dependent on moisture content (e.g., [179]).

Rocks also present a challenge. Unless expensive core is available (e.g., [170]) then drill cuttings must be used instead. Similar to granular soils, this leads to difficulty in reconstitution and moisture contents will not be representative of in situ conditions. For example, the dry rock cuttings tested in Reference [171] show a large deviation from the in situ TRT results.

### 5.1.4. Error Sources from In Situ Test Data

As discussed in Section 4.2, one of the main sources of error in thermal response testing is the transfer of energy from the test equipment to the ambient air conditions before the circulating fluid has had a chance to reach the ground. This happens if the rig and connecting pipes are not properly insulated, or the length of the connecting pipes is not minimised [108]. Where information is available, it appears that the majority of tests reported in Table A3 were conducted in scenarios where the fluid injection temperature was higher than the surrounding air temperatures. This means a tendency for heat loss to the air and an underestimation of thermal conductivity due to overestimation of the actual heat transferred to the ground. Obviously, when tests are conducted on especially warm days, or where there is a heat rejection test, then the opposite phenomena may occur.

Another potentially systematic source of error for thermal response tests is particularly relevant for energy piles. As discussed in Section 4.4, simple interpretation methods applied to low aspect ratio pile TRTs will systematically overestimate the thermal conductivity. This feature can also be observed in Figure 19, where the smallest aspect ratio pile tests show some of the greater laboratory to field data differences (e.g., [47,172,173]).

### 5.2. Example Characterisation

An example of the challenges of thermal conductivity characterisation across these scales is shown in Figure 20, which presents test results from a site in Belgium. The site contains five energy test piles and a borehole heat exchanger (BHE) as well as other boreholes and cone penetration test (CPT) locations [180]. The thermal conductivity at the site was determined by both laboratory testing and a thermal response test on the BHE. Samples were taken from different depths in the same hole. Undisturbed samples were tested with the needle probe. The disturbed samples were reconstituted and tested with a transient plane source probe at different voids ratios, assuming fully saturated conditions. These results are presented in Figure 20, along with the range of results from the borehole TRT. The results vary by almost a factor of 2 and reflect uncertainties arising from sample quality, derived characterisation from disturbed samples, errors from the use of a short borehole, as well as the overall heterogeneity of the site as shown by the CPT profiles.

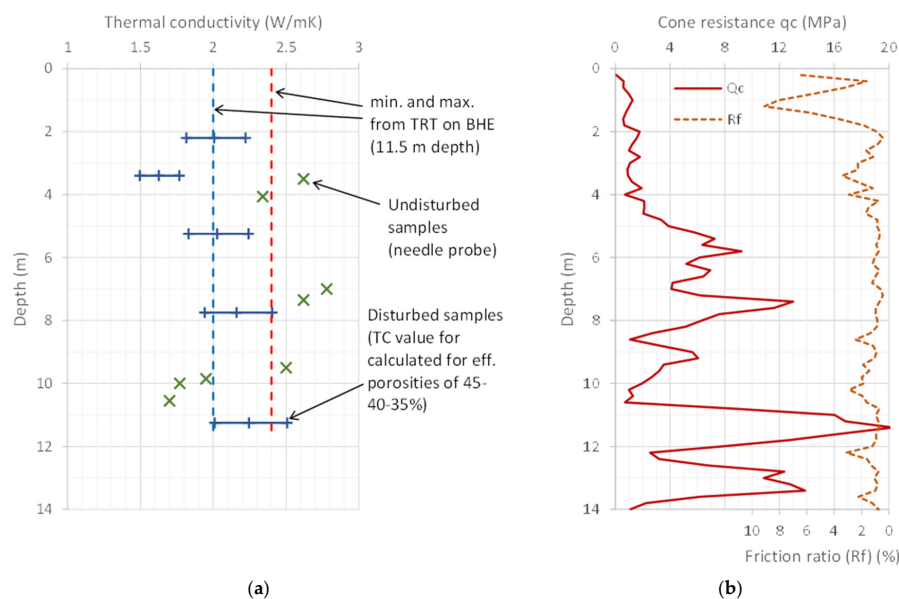


**Figure 20.** Soil characterisation of a site in Ostend, Belgium, showing: (a) thermal conductivity values from disturbed and undisturbed samples and from a TRT on a 11.5-m-deep borehole; (b) cone resistance and friction ratio profiles. Based on data from the Smart Geotherm project funded by the agency Flanders Innovation and Entrepreneurship.

### 5.3. Upscaling from Field to Regional Scale

It is desirable to have a general knowledge of the spatial distribution of the geothermal characteristics of an area before determining in detail the design parameters for a shallow geothermal facility [181]. Consequently, the question of upscaling local data, whether collected in situ through TRT or via laboratory studies on samples, to regional information has become important. The use of such datasets in a geographical information system (GIS) interactive online platform is becoming common. An example is the Thermomap project, which mapped the very shallow geothermal potential (up to a depth of 10 m) across Europe [182]. However, reliable large-scale geothermal mapping can only be based on a significant number of individual in situ or laboratory measurements of thermal conductivity [183].

Taking a regional example in more detail, for Flanders (Belgium), thermal conductivity maps were developed and integrated in an online geothermal screening tool (<http://tool.smartgeotherm.be>). An existing hydrogeological model of the area was used as a basis. All soil layers were classified by their lithostratigraphic description and subdivided into five soil categories (sand, clayey sand, loam, sandy clay, and clay). Next, two subsets of minimum and average thermal conductivity values were defined for the five soil categories by a calibration process that aimed to underestimate the in-field thermal conductivity by only 5% for the minimum values and 50% for the average values. This calibration was based on 14 available TRT results. Figure 21 shows the derived average thermal conductivity map for a depth of 100 m or up to bedrock. Subsequently, six new TRT results were gathered and compared to the minimum and average predicted values, respectively. All measured thermal conductivity values were higher than the minimum predicted values and five of the six average predicted values lie in the  $\pm 10\%$  deviation band of the measured thermal conductivity value.

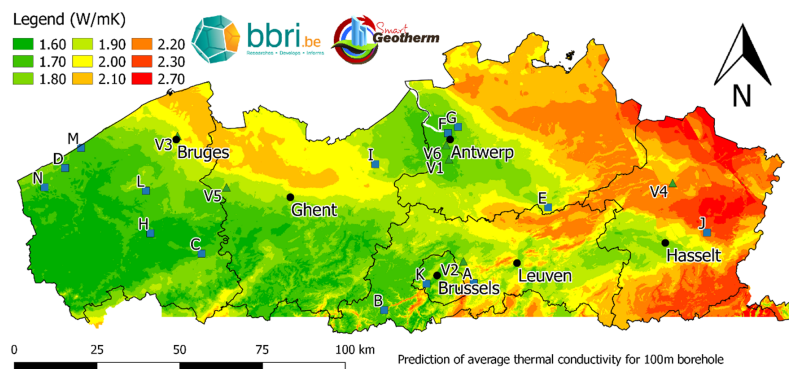


**Figure 21.** Prediction of the average thermal conductivity in Flanders over a depth of 10 m or up to bedrock. The available TRT results for thermal conductivity calibration are indicated by letters A to N. The TRT results used for verification of the maps are indicated by V1 to V6.

## 6. Characterisation of Thermo-Hydro-Mechanical (THM) Soil Behaviour

### 6.1. Relevant Coupling Effects in Energy Geostructures

While ground thermal characterisation has already been discussed above, the issues of ground mechanical and hydraulic effects induced by temperature changes are addressed in this section.

During the operation of SGE systems, soil temperature varies typically in the range of 5 °C to 40 °C (e.g., [184]). Laboratory test results in those temperature ranges are available in the literature (e.g., [26,185,186]). However, most of the experimental evidence dealing with THM soil behaviour is related to radioactive waste disposal problems, and involve much wider temperature ranges, typically from 20 °C to 100 °C (e.g., [23–25]). Other geomechanical/geophysical topics where soil THM behaviour is relevant include the analysis of catastrophic landslide collapse (e.g., [187–190]), rapid slip events in faults (e.g., [191,192]), and the effects of freezing-thawing cycles on soil mechanical



properties (e.g., [193–195]). However, overall, there is a relative lack of experimental data on soil THM behaviour, although the scientific community has acknowledged the importance of this subject for several engineering applications.

The issue of mechanical effects due to thermal loads on SGE applications is relevant to all energy geostructures (energy piles, diaphragm walls, or tunnel linings), as THM effects should be accounted for in addition to structural design loads. On the other hand, BHE are excluded from thermo-mechanical analyses, given their purely thermal function.

The magnitude of additional stresses and strains resulting from temperature variations on energy geostructures depends on many factors and the way they mutually interact. Among the most important factors are the transient heat conduction parameters (as they determine the temperature field), the contrast between the volumetric elastic thermal expansion coefficients of the different phase constituents of the soil (solid, liquid, and gaseous) and of concrete, saturation ratios and permeability, the drainage conditions, and the structure's boundary constraints.

Due to its microstructure (multiphase constitution), soil shows a complex THM behaviour, in which particle size, mineralogy, and stress history play major roles. In normally consolidated clayey soils under constant mechanical load, heating induces thermo-plastic loading and contractive volumetric behaviour, while heavily over-consolidated clays tend to exhibit a thermo-elastic response (although according to some authors, inelastic strains can also be observed [196]). This behaviour has been successfully captured by constitutive modelling in the framework of Cam-Clay, including the thermal dependency of the soil volumetric behaviour, upon formulating a temperature-dependent hardening rule ([24,25,197–199]) followed by experimental confirmation (e.g., [198,200]).

A number of unclear aspects about the mechanical effects of thermal cycling on SGE systems are still to be studied ([201,202]), and some conflicting results emerge from the literature (e.g., [3,201]). The importance and relevance of these effects, and their influence in energy geostructure structure design, has not yet been clearly assessed. Moreover, no standard tests for soil THM characterisation have been yet identified.

A first approximation for evaluating thermo-mechanical soil response can be obtained by means of analytical solutions assuming several simplifications (e.g., [200]) which imply the evaluation of an elastic thermal expansion coefficient. Greater insight can be obtained by carrying out typical soil mechanics laboratory tests, properly adapted to temperature-controlled conditions (e.g., [184,186,203,204]).

## 6.2. Effect of Temperature on Soil Mechanical Behaviour

By virtue of soil's multiphase nature, to model THM effects the behaviour of the different constituents must be taken into account. Between the upper- and lower-bound saturation, namely the completely dry and fully saturated conditions, the partially saturated soil conditions introduce additional complexity, especially for fine grained soils, due to the presence of suction forces that are also temperature dependent. Non-isothermal partially saturated soil conditions will not be addressed here, but the interested reader is referred to, e.g., References [205–207] for further reading.

In the simplest case of an elastic isotropic soil element in unrestrained and saturated conditions (free expansion), the volumetric strain rate  $\epsilon_v^T$  (volumetric thermal expansion) due to an applied temperature rate  $T$  can be obtained analytically by:

$$\epsilon_v^T = -\beta T, \quad (5)$$

where  $\beta$  is the volumetric free thermal expansion coefficient for any drainage condition (including partially drained conditions) obtained through [199]:

$$\beta = \frac{[K + (1 - n)K_f]\beta_g + K_f(n\beta_w - \zeta/T)}{K + K_f}. \quad (6)$$



In the above,  $\beta_g$  and  $\beta_w$  are the volumetric thermal expansion coefficients of the soil particles and water, respectively;  $K$  and  $K_f$  are the bulk modulus of the soil skeleton and Biot's modulus, respectively;  $n$  is the porosity ( $K_f = K_w/n$ ,  $K_w$  the water's bulk modulus); and  $\zeta$  is the rate of water per unit volume flowing into or out of the soil voids ( $\zeta > 0$  for water flowing out of the voids). Thus, four constants enable the estimation of the elastic soil thermal expansion.

For the same conditions, the excess pore pressure rate may be obtained as [199]:

$$u = \frac{KK_f[n(\beta_w - \beta_g) - \zeta/T]}{K + K_f}T. \quad (7)$$

In undrained conditions,  $\zeta = 0$ . For totally drained conditions ( $K_f = 0$  or  $\zeta = n(\beta_w - \beta_g)T$ ),  $\beta = \beta_g$  and no pore pressure develops ( $u = 0$ ). In the other cases, and when  $\beta_w \neq \beta_g$ , a change in pore pressure occurs. The trend is such that under an increase in temperature ( $T > 0$ ), if the thermal expansion coefficient of the fluid ( $\beta_w = 2 \times 10^{-4} \text{ }^\circ\text{C}^{-1}$ , at  $20 \text{ }^\circ\text{C}$ ) is higher than that of the solid grains (as generally happens), the soil skeleton restrains the water expansion and the pore pressure increases, and consequently the effective stress (and the soil strength) decreases. The opposite occurs under a decrease in temperature. This effect of pore water increase during heating is known as thermal pressurisation (e.g., [188,191,192,208,209]).

Whenever the thermo-mechanical loading and soil conditions are such that irreversible (i.e., plastic) straining occurs, the above relationships are not sufficient to capture the constitutive soil behaviour and reference should be made instead to elasto-plastic relationships. To calculate thermo-plastically induced strain (in a stress- and temperature-controlled problem) or stress (in a strain- and temperature-controlled problem), employing a critical state-type constitutive model it is typically necessary to numerically solve a system of rate equations (e.g., [24,188,210]).

Along the same lines, formulations exist to calculate thermal pressurisation in thermo-plastic conditions, e.g., when the soil's solid skeleton exhibits thermo-plastic volumetric collapse while pore water still tends to expand thermo-elastically. Thermo-plastically induced pore pressure build-up can be obtained either via assuming a constant pressurisation coefficient (e.g., [187]) or by considering a temperature-dependent pressurisation coefficient, allowing for gradual soil skeleton collapse (e.g., [188]).

### 6.3. Laboratory THM Characterisation

Laboratory THM soil characterisation has been more intensively studied in the last two decades; however, a number of seminal works on the THM behaviour of clays has been carried out before (e.g., [24,197,211,212]). Typically, laboratory THM soil characterisation is carried out by adapting standard laboratory soil testing devices to non-isothermal conditions, mainly oedometer, direct/simple shear, and triaxial devices, and more recently by means of centrifuge modelling [213]. The temperature controlled triaxial test is one of the best-established approaches for characterising THM behavior due to its relative simplicity and capability to control key variables. With the aim of studying the behaviour of SGE applications, both monotonic and cyclic thermal loading (aimed at reproducing seasonal temperature cycles) have been applied to soil samples in different experimental setups.

Laloui et al. [26] identified the main issues related to laboratory thermo-mechanical testing, namely developing adequate heating systems, insulation and accounting for thermal losses, thermal calibration, control of boundary conditions, and representing long-term cyclic behaviour. They also categorised thermomechanical tests in three main groups, namely those involving heating by circulating fluid, heating with internal heaters, and heating with external heaters. The interested reader is referred to Reference [26] for further details on experimental issues.

It can be observed that temperature changes may exert three major mechanical effects on soils: thermo-elastic expansion of soil particles and pore water (Section 5.2), thermo-plastic bulk volume changes, and thermally induced modification of frictional strength. This implies the possible

presence of both elastic and plastic thermally induced strains and thermal consolidation (e.g., [25,200]). Irreversible thermal effects that are most relevant to SGE systems include thermally induced strength changes and thermal consolidation.

### 6.3.1. THM Response by Triaxial Tests

Triaxial tests are particularly important in the study of THM soil behaviour, as they (also) enable the assessment of volumetric thermal expansion at constant isotropic stress. Reference [200] carried out thermal tests in isotropic conditions on a saturated illite subjected to a temperature increase from 18.9 °C up to 60 °C, followed by cooling to 18.9 °C under constant total stress of 200 kPa, in both drained and undrained conditions. The results clearly show the combined effect of elastic and plastic behaviour on the temperature-volume-effective stress test results (Figure 22). In drained conditions, the increase in temperature leads to increasing compressive volumetric strains and an expulsion of water from the clay sample, whereas with a decrease in temperature the reverse occurs. A tangent thermal expansion coefficient can be obtained at each point. In undrained conditions, heating produces a pore pressure increase and, consequently, an effective stress decrease.

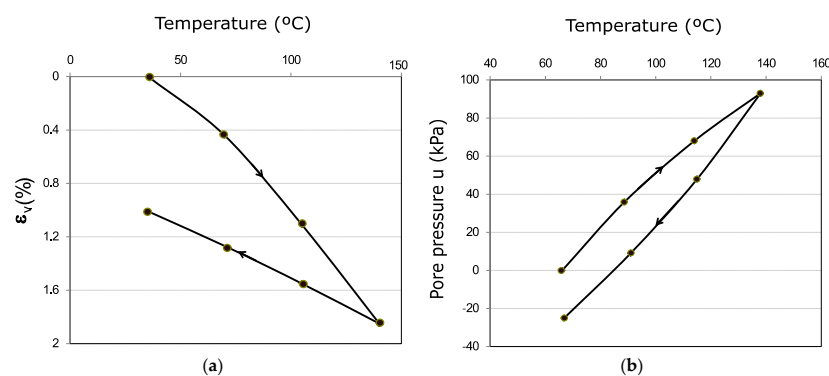


**Figure 22.** Volumetric strain (a) and pore pressure change (b) in undrained conditions for saturated illite under a constant total stress of 200 kPa as a function of temperature (adapted from Reference [200]).

It should be noted that two plastic effects interact during heating at constant mean effective stress: a softening effect due to a higher temperature (shrinkage of the yield surface), and a hardening effect due a reduction in void ratio (thermal compaction). Due to changes in the particle arrangement, the process is not reversible during cooling for soils normally or slightly over-consolidated, and residual strains remain.

In Reference [25], the thermomechanical response of kaolin was tested in isotropic stress conditions by means of a triaxial device with controlled temperature (Figure 23). The adaptations of the system to non-isothermal conditions are described in detail in Reference [203].

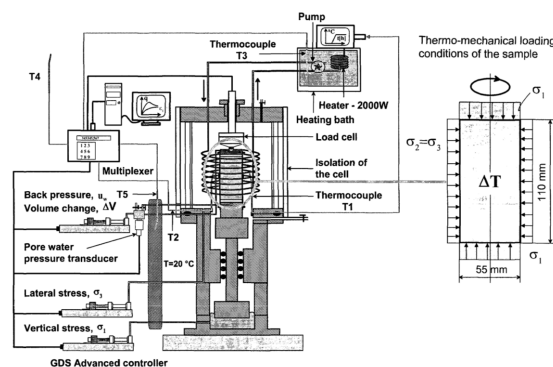


**Figure 23.** Triaxial device with controlled temperature [203].

Very illustrative results are shown in Figure 24, where it is observed that the samples tested in normally consolidated or slightly over-consolidated conditions exhibit irreversible compaction and density increase during drained heating (thermal hardening). In over-consolidated conditions, during drained heating, clayey soils initially show a dilatant behaviour (due to thermo-elastic dilation), possibly followed, for higher temperatures, by thermo-plastic volume reduction.

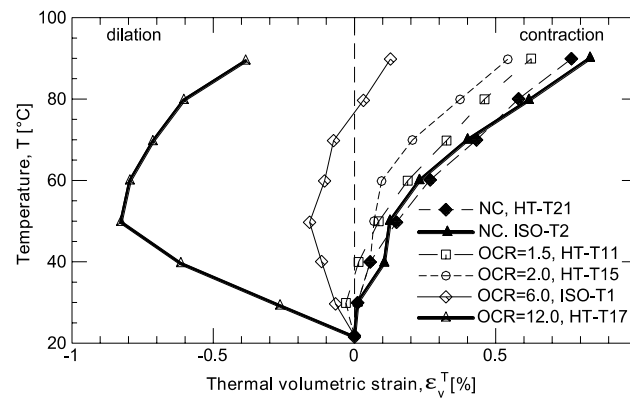


**Figure 24.** Thermal volumetric strain of speshwhite Kaolin clay during drained heating from 22 °C to 90 °C [25].

The transition from contractive to expansive behaviour depends on the over-consolidation ratio (OCR) and on the soil type. Figures 25 and 26 show the evolution of volumetric strains with OCR and clay activity, respectively. It can be deduced that the higher the activity, the higher the potential for thermal volume change.

The effect of temperature on soil mechanical behaviour under general axisymmetric states has also been studied by means of triaxial tests (e.g., [24,212,214]). The tendency and magnitude of the shear strength change for different temperatures reportedly depends on a variety of factors, such as soil type, mineralogy, OCR, drainage conditions, and thermal rate. Reference [215] emphasised the importance of previous mechanical and thermal loading. In fact, in drained conditions, in some cases heating causes strengthening in clays (thermal hardening) and a stiffer behaviour can be observed during subsequent shearing. This hardening effect (associated with increasing shear strength) in drained conditions was confirmed by Reference [216], who subjected soil samples to heating before shearing them in undrained conditions.

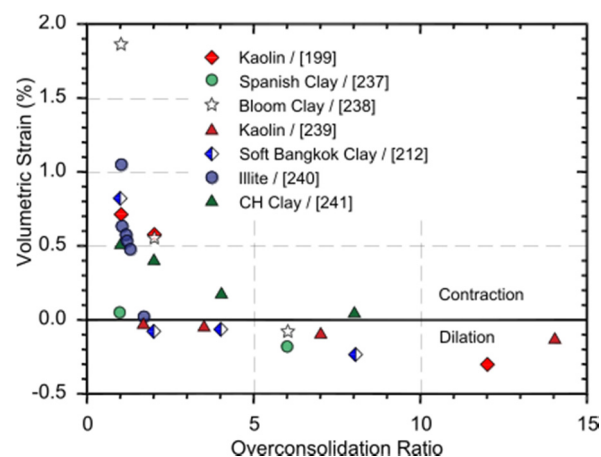


**Figure 25.** Evolution of volumetric strain with the over-consolidation ratio (OCR) for clays ( $\Delta T = 20\text{--}40\text{ }^{\circ}\text{C}$ ) (adapted from Reference [26] using data from References [203,216–221]).

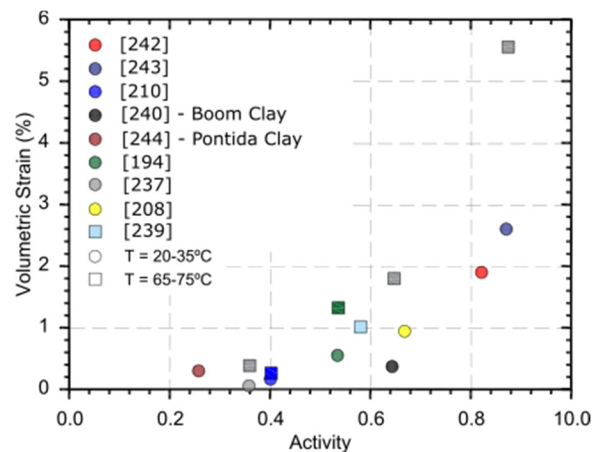


**Figure 26.** Evolution of volumetric strain with clay activity (adapted from Reference [26] using data from References [198,212,214,217,219,220,222–224]).

### 6.3.2. THM Response by Shear Tests

The direct shear test measures the shear strength properties of soils or soft rocks along a predetermined plane. The test is carried out on a soil sample placed in a square cross-section metal box. The box is split horizontally at mid-height and a small clearance is kept between the two halves of the box. The soil sample is sheared by moving the top half of the box relative to the bottom half. The rate of strain can be varied to obtain drained or undrained conditions, depending on whether the strain is applied slowly enough to prevent pore-water pressure build-up or not. However, a specimen's pore pressure cannot be measured in standard direct shear apparatus. The adaptation of this test to non-isothermal conditions is relatively simple and the main concern is to maintain constant temperature conditions during the test. Due to its configuration, this test has been used to investigate the behaviour of the pile-soil interface, which is particularly important to assess the response of floating energy piles. Sand-concrete and clay-concrete interfaces were tested in this way under constant normal load and constant normal stiffness conditions monotonically and cyclically.

In Reference [225], a direct shear device developed and calibrated for non-isothermal soil-structure interface testing was used, adopting a heating system composed by an electrical resistance, an electrical power supplier, an insulation system, and a thermocouple.

The main conclusions of Reference [225] were that the sand-concrete interface was affected by cyclic shear strength degradation but not directly by temperature. The concrete-clay interface appeared to be sensitive to thermal variations, showing an increase of clay-pile interface strength upon thermal loading, probably because of thermally induced compaction strength with increasing temperature (thermal consolidation).

To investigate the shear behaviour of sand, clay, and soil/concrete interface, Reference [184] carried out shear tests under very small normal stresses (5–80 kPa) at various temperatures (5 °C, 20 °C, and 40 °C) in a direct shear apparatus, equipped with temperature control. A schematic of the system is shown in Figure 27. A copper tube was accommodated in the shear box container and connected to a heating/cooling circulator, able to impose a temperature in the range of −20 °C to 80 °C. Two thermocouples were installed in the box: one below the shear box and the other at the water surface. The container was thermally insulated using expanded polystyrene sheets. The soil (or soil/concrete) was placed between two porous stones and two metal porous plates. The authors conclude that in the investigated temperature range, thermally induced effects on strength are negligible.

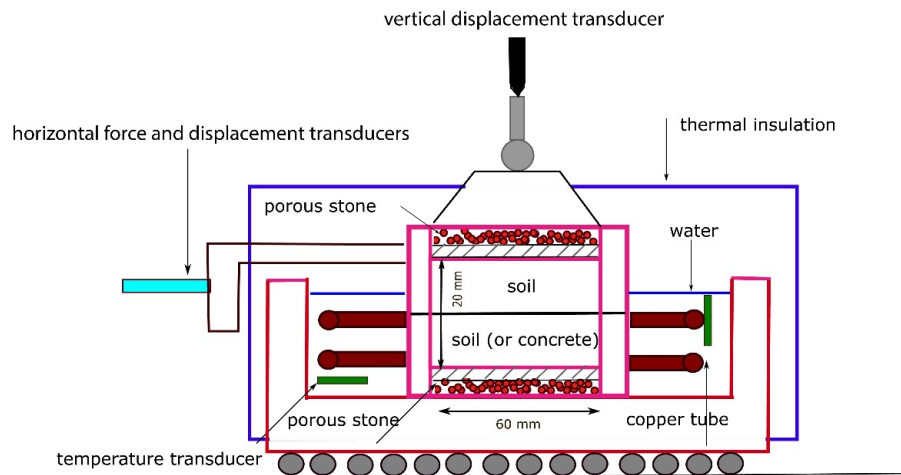


**Figure 27.** Direct shear apparatus with temperature control system (adapted from Reference [184]).

Recent studies using shear tests devices to assess the effect of temperature by means of monotonic and cyclic loading do not present totally convergent conclusions. Furthermore, it should be noted that this test is less reliable than others—due, for example, to the lack of information on the complete stress state of the tested specimen and the need to impose the orientation of the shear surface.

### 6.3.3. THM Response by Oedometric Tests

The oedometer test allows characterising the soil stress-strain behaviour of saturated specimens under one-dimensional compression, and can be used to determine compressibility and consolidation parameters. The temperature-dependent behaviour of soil under oedometric loading (vertical loading and prevented lateral deformation) has been studied for some decades (e.g., [185,186,226,227]). These authors noticed a significant temperature effect on the compressibility of the tested clays. For increasing temperature, soil compressibility tends to increase and the pre-consolidation pressure decreases (shrinkage of the yield surface), causing the compression curve to move towards smaller effective stresses.

More recently, with the specific aim of studying SGE applications, the response of a natural silty clay soil to thermal loading in drained conditions was investigated by means of oedometer tests by References [228] and [225]. The devices employed for the experiments are oedometer cells that were adapted to include temperature control (see Reference [204], and Figure 1 therein). Thermal load is provided by spiral tubes placed around the specimens and connected to a heater (the temperature of the bath being imposed through a thermostat). A pump circulates the water at the desired temperature inside the spiral tubes, from the thermo-controlled bath to the cells. During the tests, the temperature is monitored inside each cell using four thermocouples. The cells are insulated with a polystyrene box to minimise thermal losses [204].

The abovementioned tests were carried out at various constant temperatures, aimed at analysing the soil sensitivity to temperature and thermal cycling under constant vertical effective stress. Temperature ranged between 5 and 60 °C. In normally consolidated conditions it was observed that after a couple of thermal cycles (between 5 and 60 °C), the irreversible volumetric strains stabilised between 0.5 and 1%, with the following cycles being reversible. On the other hand, in over-consolidated states, the samples showed no irreversible volumetric strain, leading the authors to confirm that over-consolidated soils develop essentially elastic behaviour during heating. As expected, silty clay specimens tested under normal consolidation conditions ( $OCR = 1$ ) exhibited thermo-plasticity, showing that most of the irreversible deformation occurred during the first heating-cooling cycle. The results of two such oedometer tests run at 20 °C and 40 °C are shown in Figure 28. It is clear that the soil undergoes a reduction in the elastic domain size with increasing temperature. In the same

figure, the response is shown of a sample submitted to thermal cycling, which induced a thermal consolidation effect.

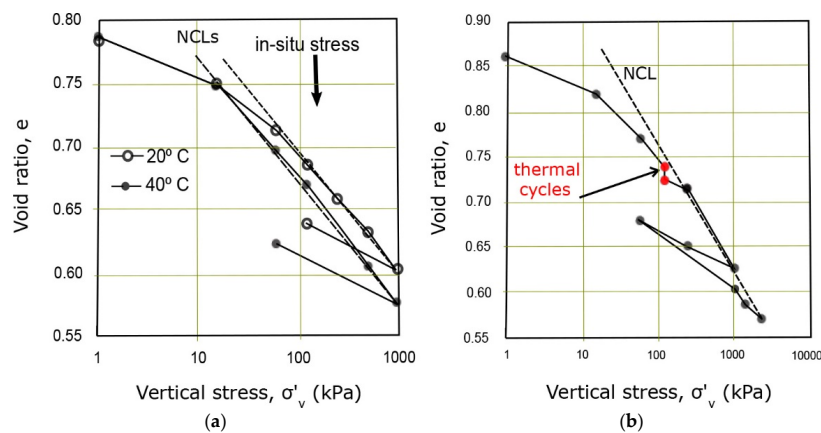


**Figure 28.** Oedometric results (a) tests at 20 °C and 40 °C samples; (b) test results with thermal cycles (adapted from Reference [204]).

#### 6.4. Basic Parameters Needed for Thermo-Mechanical Modelling

To be able to reproduce the observed thermo-mechanical behaviour of soils and eventually make predictions in boundary value problems involving SGE systems, one should typically resort to finite element modelling, incorporating a suitable constitutive law that can capture the most significant thermo-mechanical effects. To that aim, constitutive formulations exist such as those based on the Critical State Soil Mechanics framework (cf. Section 6.1), that can be easily incorporated into commercial finite element codes. Upon referring to one of the simplest such thermo-mechanical constitutive formulations, as that presented by Reference [198], it can be deduced that a basic set of parameters needed to reproduce a soil's basic thermo-mechanical behaviour (in addition to standard Cam Clay parameters) consists of: (a) volumetric thermo-elastic expansion coefficient, (b) thermo-plastic softening parameter, and possibly (c) a parameter describing thermally induced changes in the Critical State parameter  $M$  [229].

Of the above, parameter (a) is the best established and can be measured by means of different experiments, such as performing drained heating tests at constant isotropic stress in over-consolidated specimens (e.g., [198,230]). Parameter (b) describes the rate at which thermal softening occurs, i.e., the thermal dependency of the soil's apparent pre-consolidation stress, defining the 'shrinkage' of elastic domain with increasing temperature. This parameter has been shown to depend upon the material type, and can be measured by means of isotropic heating tests of normally consolidated specimens in a triaxial apparatus ([198] and Figure 7 therein). Parameter (c), aimed at describing temperature effects on the frictional strength of the material, could be measured by carrying out a set of triaxial tests at different constant temperatures. However, this soil property is less well established, as somewhat contradictory results emerge from the literature. For example, while Reference [229] proposed that the Critical State parameter  $M$  may exhibit a linear decreasing relationship with increasing temperature, other studies (e.g., [212,215]) suggested that  $M$  tends to increase or remain constant with increasing temperature. Hence, at least for basic thermo-mechanical analyses, it is suggested not to consider  $M$  to vary with temperature.

The above parameter determination suggestions are by no means exhaustive of the wide range of possible thermo-mechanical soil features that may be of academic interest. For example, including rate dependency, thermal cycling, and thermal pressurisation effects would require more complex models and the consequent increase of the number of parameters to be determined, in addition to standard parameters within the Cam Clay framework. However, the above outlined simple framework



provides some didactic insight into the basic features that should be considered and the corresponding parameters when approaching a thermo-mechanical problem for SGE applications.

## 7. Discussion and Conclusions

Soil and rock thermal characterisation is essential for an appropriate energy assessment of SGE systems. As the scope of SGE systems has expanded to include energy geostructures and other novel heat exchangers, so the required range of parameters required for design has correspondingly increased. As a consequence, there is a move from the determination of thermal conductivity to include the quantification of coupled thermo-hydro-mechanical behaviour; with it, the degree of uncertainty in parameter estimation increases.

However, even when considering the relatively simpler assessment of thermal conductivity, there are many pitfalls and challenges arising from the nature of soils and rocks as three phases materials. It is particularly important to understand when thermal processes other than diffusion may be occurring within the material being tested. Soil thermal conductivity can be determined in the laboratory or in the field. The advantage of laboratory testing is the speed and therefore relatively low costs. However, there may be difficulties with sampling quality and representative sample preparation as well as the scale and thermal conditions of the tests compared with in situ field conditions. While large-scale TRT is arguably more representative of the true conditions of a SGE system, it is time-consuming, expensive, and provides only a lumped understanding of the ground behaviour. This paper presents a first systematic comparison between both field and laboratory testing and different approaches to laboratory testing.

Laboratory tests can be steady-state or transient in terms of the heat flow conditions. Steady-state tests require good experimental design to prevent excessive heat losses. They also require a relatively long durations (hours) which means that moisture migration can occur in partially saturated samples. While transient tests (which occur in minutes) overcome both of these issues, they test a small and hence less representative volume of soil. For the most common approach, the needle probe, there can also be problems when testing large grain sizes, and hard clays or rocks where predrilling may lead to additional errors. This has led to recent developments of transient plane source heat probes which are becoming increasingly popular, but for which there is limited systematic critical and comparative assessment.

Where comparisons between steady-state and transient approaches have been made, they typically include the hot guarded plate and the needle probe. Often different studies appear contradictory, but careful examination does reveal some trends. For dry sands, a good match is usually obtained since thermal processes other than conduction are rarely occurring. For partially saturated fine soils, steady-state methods can overestimate the thermal conductivity if excessive heat losses occur, but it is perhaps more likely to underestimate due to moisture migration and sample drying. Drying can also be seen in some sands. Finally, when saturated sands and gravels are tested at elevated temperatures, steady-state tests can overestimate thermal conductivity due to the presence of buoyancy-driven flow in the pore spaces.

These results suggest that transient testing is preferable for fine sources and partially or fully saturated sands. Steady-state testing is acceptable for dry sands and will be necessary for coarser soils. Rocks and hard clays would be most suited to steady-state tests, or if there is concern about partial saturation in the clays, then transient plane sources techniques can be applied.

While soil and rock thermal laboratory testing has long been of interest for a variety of academic and practical fields, in situ thermal response testing may constitute the principal development in the field of soil thermal characterisation related specifically to SGE applications. Together with the estimation of the effective thermal conductivity over the full scale of the ground heat exchanger, it also provides the thermal resistance of the heat exchanger. A limitation of the standard TRT practice is that it yields an averaged value of the thermal conductivity of the soil, which may prevent the optimisation of the energy design. Recently, enhanced and distributed TRT techniques, providing continuous

in-depth soil thermal characterisation, have been developed to counter this. These approaches require additional equipment and therefore expense, but provide additional information that may assist in guiding the heat exchanger length. This paper provides a first comparison of TRT and DTRT techniques and finds the results to be broadly comparable, albeit with higher values from the DTRT in some cases. This could be due to the greater significance of non-radial heat flow when the heat exchanger is split into many smaller lengths. Currently DTRT remains mainly a research tool, with most routine tests operating a standardised procedure. However, it could be valuable in circumstances when the geological conditions are known to be heterogeneous. Developments in TRT techniques also include TRT for pile heat exchangers, whose interpretation requires more advanced models that consider the low aspect ratios and unique geometries of the foundation piles. Basic interpretation methods are shown to systematically overestimate thermal conductivity and are not advised. As a consequence, pile TRTs are not recommended in routine practice without the commitment to more time-consuming analyses such as numerical simulation.

There is also a tendency for systematic differences to arise between field and laboratory scale determinations of thermal conductivity. Overall, field testing is shown to consistently give higher results for thermal conductivity. However, many different factors may lead to these discrepancies. These include issues of method such as heat losses in poorly insulated tests in the field, sample disturbance, and drying before laboratory testing. However, there are also differences due to scale effects such as strata layering and the presence of groundwater flow which can significantly enhance effective thermal conductivity in the field. Despite these differences, except for the smallest SGE schemes, TRT is always recommended since it best represents operational conditions. However, consideration of both field and laboratory data is desirable to obtain the fullest understanding of the sub-surface conditions. In the absence of a laboratory campaign, the use of a DTRT would be an alternative way to provide similar information.

For energy geostructures, where thermal loading affects the (hydro)mechanical behaviour of both soil and structure, there are significant additional challenges for thermal properties estimation. While soil thermo-hydro-mechanical behaviour has become better understood in recent years, the complexities of the accepted constitutive models mean that parametrisation of those models remains a largely academic pursuit. While the importance of the over-consolidation ratio is well understood in determining modes of behaviour, many other factors also influence the expected thermally induced strains. Consequently, and given the absence of routine commercial test methods, those conducting structural design in practice will no doubt be required to make assumptions and potentially derive material parameters from the academic literature. Bridging this gap remains the largest current challenge for the research community and will need to progress in parallel with the development of appropriate design methods.

**Acknowledgments:** The authors gratefully acknowledge Transport and Urban Development COST Action TU1405—European Network for Shallow Geothermal Energy Applications in Buildings and Infrastructures (GABI; [www.foundationgeotherm.org](http://www.foundationgeotherm.org)).

**Author Contributions:** This manuscript was planned in the aim of Working Group 1 (Soil Thermal Characterisation) of GABI COST Action (TU1405). Ana Vieira coordinated the realisation of the manuscript and was responsible for Section 6. Section 3 was supervised by Paul Cristhodoulides, Section 4 by Saqib Javed and Section 5 by Fleur Loveridge. The 7 first authors formed an editorial group which has worked closely together in the final production stages and constitute the main authors of the manuscript, which has been further reviewed by Fleur Loveridge. All authors provided technical, theoretical and practical support and reviewed and approved the final version.

**Conflicts of Interest:** The authors declare no conflict of interest.

## Abbreviations

The following acronyms and nomenclature are used in this manuscript.

### Acronyms

|    |                              |
|----|------------------------------|
| 1U | Single U pipe heat exchanger |
| 2U | Double U pipe heat exchanger |

|        |  |
|--------|--|
| 3U     | Three U pipe heat exchanger                                      |
| APGE   | Auger Pressure Grouted Energy                                    |
| AR     | Aspect Ratio   |
| ASHRAE | American Society of Heating, Refrigerating, and Air-Conditioning |
| BHE    | Borehole Heat Exchanger  |
| CaRM   | Capacity Resistance Model  |
| CCM    | Composite Cylindrical Model                                      |
| CPT    | Cone Penetration Test  |
| CSM    | Cylinder Source Model  |
| DTRT   | Distributed Thermal Response Test                                |
| DTS    | Distributed Temperature Sensing                                  |
| ETRT   | Enhanced Thermal Response Test                                   |
| FDTR   | Frequency Domain Thermoreflectance Technique                     |
| FEA    | Finite Element Analysis  |
| FEM    | Finite Element Method  |
| FLS    | Finite Line Source   |
| GHE    | Ground Heat Exchanger  |
| GIS    | Geographical Information System                                  |
| GPM    | Geothermal Properties Measurement                                |
| GPM    | Geothermal Properties Measurement                                |
| ILS    | Infinite Line Source   |
| LVDT   | Linear Variable Differential Transformers                        |
| OCR    | Over-Consolidation Ratio   |
| SGE    | Shallow Geothermal Energy  |
| TC     | Thermal Conductivity   |
| TEP    | TRT Evaluation Program   |
| TG     | Thermal Grout  |
| THM    | Thermo-Hydro-Mechanical  |
| TPS    | Transient Plane Source   |
| TRT    | Thermal Response Test  |
| W      | W-shape pipe heat exchanger                                      |

### Nomenclature

|                             |  |
|-----------------------------|--|
| $\Delta$                    | increment or change operator (-)   |
| A, B, C                     | main axes of thermal conductivity with angles $\alpha$ , $\beta$ , $\gamma$ (rad or $^{\circ}$ ) to line of scanning, respectively |
| $A_i$                       | area normal to the direction of the heat flow ( $m^2$ )  |
| $D_{10}$                    | 10% of the sample is passing the 1.4 millimeter size (-)   |
| E                           | void ratio (-)   |
| K and $K_f$                 | bulk modulus of the soil skeleton and Biot's modulus, respectively (-)   |
| $L_i$                       | length of the material (m)   |
| M                           | critical state parameter   |
| N                           | porosity (-)   |
| O                           | area of the heat spot ( $m^2$ )  |
| Q                           | heat flow (W)  |
| q                           | heat rate ( $W \cdot m^{-1}$ )   |
| $q_c$                       | cone resistance (MPa)  |
| $r_b$                       | ground heat exchanger radius (m)   |
| $R_b$                       | thermal resistance of the ground heat exchanger ( $K \cdot m \cdot W^{-1}$ )   |
| $R_f$                       | friction ratio (%)   |
| S                           | detection area of the radiometer   |
| $S_r$                       | degree of saturation   |
| $T_{ambient}$ and $T_{air}$ | ambient temperature during the TRT (K or $^{\circ}C$ )   |
| $T_i$                       | temperature (K or $^{\circ}C$ )  |
| $T_{in}$ or $T_{injection}$ | inlet temperature to the ground heat exchangers during the TRT (K or $^{\circ}C$ )   |

|                         |   |
|-------------------------|---|
| $T_{out}$               | outlet temperature from the ground heat exchangers during the TRT (K or °C)   |
| $T_R$                   | reference temperature (K)   |
| $U$                     | excess pore pressure (kPa)  |
| $V$                     | velocity of scanning ( $\text{m}\cdot\text{s}^{-1}$ )   |
| $X$                     | direction coordinate or distance (m)  |
| $\alpha$                | thermal diffusivity ( $\text{m}^2\cdot\text{s}^{-1}$ ], defined as $\alpha = \lambda/\rho c_p$                        |
| $\beta$                 | volumetric free thermal expansion coefficient ( $\text{K}^{-1}$ )   |
| $\beta_g$ and $\beta_w$ | volumetric thermal expansion coefficients of the soil particles and water, respectively ( $\text{K}^{-1}$ )           |
| $\varepsilon_v$         | volumetric strain (-)   |
| $\varepsilon_v^T$       | volumetric thermal expansion (-)  |
| $\zeta$                 | rate of water per unit volume flowing into or out of the soil voids ( $\zeta > 0$ for water flowing out of the voids) |
| $\lambda$               | thermal conductivity ( $\text{W}\cdot\text{m}^{-1}\cdot\text{K}^{-1}$ )   |
| $\lambda_R$             | reference thermal conductivity ( $\text{W}\cdot\text{m}^{-1}\cdot\text{K}^{-1}$ )                                     |
| $\rho c_p$              | volumetric heat capacity ( $\text{J}\cdot\text{m}^{-3}\cdot\text{W}^{-1}$ )   |
| $\sigma'_v$             | effective vertical stress (kPa)   |
| $\sigma_i$              | principal stresses (kPa)  |

## Appendix A

This section contains Tables A1–A3.

**Table A1.** Summary of the advantages and disadvantages of each technique used for measuring soil and rock thermal properties.

| Method                            | Limitations  | Advantages  |
|-----------------------------------|--|---|
| <b>Guarded hot plate</b>          | (1) Large sample required. (2) Method not designed with soils in mind. (3) Presence of contact resistance that is difficult to evaluate or eliminate. (4) Overestimates the thermal conductivity of coarse saturated soils as it includes the effect of buoyancy-driven flow. (5) Moisture migration may occur in unsaturated soils. (6) Long duration tests.                        | (1) Standardised method [231] for rocks. (2) More suited to dried samples. (3) Possibility to measure thermal conductivity at different temperatures without needing external chambers.   |
| <b>Thermal cell</b>               | (1) Overestimates the thermal conductivity due to uncontrolled heat losses. (2) Long test durations. (3) Potential for moisture migration in unsaturated soils.  | (1) Larger thermally activated zone than transient methods. (2) Suitable for any soil. (3) Sample sizes and shape suited to routine site investigation practice.  |
| <b>Divided bar</b>                | (1) It is a comparative method. (2) Similar problems to guarded hot plate including long duration and potential for moisture migration.  | (1) Larger thermally activated zone than transient methods. (2) Well suited for rock testing.   |
| <b>Thermal needle probe</b>       | (1) Need stable applied current. (2) Small sample volume is thermally activated; hence many tests may be needed in heterogeneous soils. (3) Not appropriate when soil grain size is large relative to needle. (4) The samples need to be large enough to avoid the effect of boundaries. (5) Contact resistance errors created when hole is drilled into rock samples or hard soils. | (1) Standardised method [46]. (2) Very rapid test; minimising moisture migration and hence suitable for partially saturated samples. (3) Portable version for in situ measurements. (4) Different needle sizes available to adapt to smaller samples.   |
| <b>Thermal dual needle probe</b>  | (1) Same as limitations of the thermal needle probe, but requires extra care to ensure that insertion does not change separation of needle.  | (1) As for the thermal needle probe, but it is not standardised. (2) It can also determine thermal diffusivity.   |
| <b>Transient plane source</b>     | (1) Requires complex decision-making to select adequate sensors, power and measuring times. (2) Hard to create a smooth surface in in some soil types. (3) It is not standardised for soil and rock samples.   | (1) A wide range of sample sizes can be measured as there are different sizes of sensors. (2) Applicable to all types of soils and rocks. (3) Fast measurements. (4) Volumetric heat capacity can also be determined. (5) There is no need to drill the samples as the probe remains in contact with the surface. |
| <b>Optical scanning technique</b> | (1) It is not a standardised method for soils and rocks. (2) Not well suited to soils given the requirement for smooth polished surfaces.  | (1) Well suited for use with rocks. (2) Allows measuring the variations of the thermal conductivity along a scanning line on the sample. (3) Gives indications of the heterogeneity of the material.  |

**Table A2.** Summary of studies where thermal response testing of pile heat exchangers has been adopted to obtain the thermal conductivity of the soil.

| Pile Type, Length (m)/Diameter or Size (m) | Pipe Configuration | TRT Duration               | Interpretation Methodology                    | Pile Thermal Resistance (m.K.W <sup>-1</sup> ) | Soil Thermal Conductivity (W.m <sup>-1</sup> .K <sup>-1</sup> ) | Reference                  |
|--|--------------------|----------------------------|---|--|---|----------------------------|
| Auger pile, 25.8/0.88                      | -                  | 160 h                      | ILS *   | 0.080  | 2.40  | [232]                      |
| Auger pile, 23/0.6                         | 2U *               | 20 h                       | ILS *   | -  | 1.52  | [233]                      |
| Driven precast, 15/0.27x0.27               | 1U *               | 30 h                       | ILS *   | 0.170  | 2.56  | [234]                      |
| Driven steel tube, 17/0.244                | 1U *               | 30 h                       | ILS *   | 0.110  | 2.37  |                            |
| Auger pile APGE *, 18.3/0.305              | 2U *               | 96 h                       | ILS * initial 10 h neglected                  | -  | 2.91  | [235]                      |
| Auger pile APGE *, 18.3/0.305              | 1U *               | 67 h                       | ILS * initial 10 h neglected                  | -  | 2.98  |                            |
| Auger pile APGE *, 18.3/0.457              | 2U *               | 100 h                      | ILS * initial 10 h neglected                  | -  | 2.92  |                            |
| Auger pile APGE *, 18.3/0.457              | 1U *               | 110 h                      | ILS * initial 10 h neglected                  | -  | 3.27  |                            |
| Hollow precast pile, 13.25/0.4             | W *                | 14 h                       | 72 h 3D FEM * simulation                      | 0.131  | 2.46  | [163]                      |
| Hollow precast pile, 13.75/0.4             | 3U *               |                            |   | 0.098  | 2.53  |                            |
| Auger pile, 6/0.30                         | 1U *               | 9.5 h                      | ILS *   | -  | 2.87  | [174]                      |
|  |                    |                            | GPM *   | -  | 2.94  |                            |
|  |                    | 10 h recovery              | Recovery data                                 | -  | 2.60  |                            |
| Auger pile, 14.2/0.25                      | 1U *               | 13 h                       | ILS *   | -  | 3.23  |                            |
|  |                    | 6 h recovery               | Recovery data                                 | -  | 3.53  |                            |
| Auger pile cement/sand, 30.5/0.254         | 1U *               | 48–60 h                    | ILS *, FLS *, CSM *                           | 0.230  | 1.95–1.96–1.94  | [236]                      |
| Auger pile cement/sand, 30.5/0.254         | 2U *               | 48–60 h                    | ILS *, FLS *, CSM *                           | 0.120  | 2.02–2.02–2.03  |                            |
| Auger pile cement/sand, 30.5/0.254         | 1U *               | 48–60 h                    | ILS *, FLS *, CSM *                           | 0.220  | 1.95–1.96–1.92  |                            |
| Auger pile cement, 30.5/0.254              | 1U *               | 48–60 h                    | ILS *, FLS *, CSM *                           | 0.190  | 1.99–1.98–1.96  |                            |
| Auger pile TG *, 18.3/0.305                | 2U *               | 94 h                       | ILS * time superposition                      | -  | 2.50  | [152] with data from [235] |
| Auger pile APGE *, 18.3/0.305              | 2U *               | 96 h                       | ILS * time superposition                      | -  | 2.80  |                            |
| Auger pile APGE *, 18.3/0.457              | 2U *               | 100 h                      | ILS * time superposition                      | -  | 2.60  |                            |
| Auger pile 18.3/0.305                      | 2U *               | 96 h                       | G-function time superposition                 | 0.061  | 3.10  | [237] with data from [235] |
| Auger pile 18.3/0.305                      | 1U *               | 67 h                       | G-function time superposition                 | 0.104  | 2.98  |                            |
| Auger pile 18.3/0.457                      | 2U *               | 100 h                      | G-function time superposition                 | 0.104  | 3.18  |                            |
| Auger pile 18.3/0.457                      | 1U *               | 110 h                      | G-function time superposition                 | 0.135  | 3.77  |                            |
| Auger pile, 26.8/0.3                       | 1U *               | 34.25 days multi stage TRT | G-functions                                   | 0.125  | 2.4   | [166]                      |
|  |                    |                            | ILS *   | 0.125  | 2.6   |                            |
| Auger pile, 16.1/0.6                       | 1U *               | 72 h                       | ILS *   | -  | 4.19  | [238]                      |
|  | 3U *               | 216 h                      | ILS *   | -  | 3.75  |                            |
|  | 3U *               | 1248 h                     | ILS *   | -  | 4.99  |                            |
| Auger pile, 45/0.6                         | W *                | 48 h                       | ILS *   | -  | 2.96  | [157]                      |
|  |                    |                            | CCM *   | -  | 2.42  |                            |
| Auger pile, 18/0.42                        | W *                | 96 h                       | ILS *   | 0.370  | 2.78  | [239]                      |
| Auger pile, 15.2/0.61                      | 2U *               | 498 h                      | ILS *   | -  | 1.90–2.10   | [173]                      |
| Auger pile, 15.2/0.61                      | 2U *               | 498 h                      | Based on thermistor measurements in boreholes | -  | 2.00–2.30   | [240]                      |
| Driven precast, 15/0.3x0.3                 | W *                | 96 h                       | 2D FEM * simulation                           | 0.062  | 2.41  | [168]                      |
| Auger pile, 16.1/0.6                       | 1U *               | 72 h                       | 2D FEM *                                      | -  | 1.80  | [241]                      |
| Driven precast, 10/0.27x0.27               | 1U *               | 275 h                      | ILS *   | 0.191  | 2.74  | [242]                      |
| Micro-pile, 12/0.18                        | -                  | 96 h                       | ILS *   | 0.300  | 0.90  | [243]                      |



Table A2. Cont.

| Pile Type, Length (m)/Diameter or Size (m) | Pipe Configuration | TRT Duration | Interpretation Methodology | Pile Thermal Resistance (m.K.W <sup>-1</sup> ) | Soil Thermal Conductivity (W.m <sup>-1</sup> .K <sup>-1</sup> ) | Reference |
|--|--------------------|--------------|----------------------------|--|---|-----------|
| Driven precast, 17/0.35x0.35               | 2U *               | 120 h        | ILS *                      | 0.160  | 2.70  | [175]     |
| Auger pile, 20/0.62                        | 2U *               | 110 h        | CaRM *                     | -  | 1.50  | [160]     |

\* TG: Thermal Grout; APGE: Auger Pressure Grouted Energy; 1U: Single U; 2U: Double U; 3U: Triple U; W: W-shaped; ILS: Infinite Line Source; GPM: Geothermal Properties Measurement; CCM: Composite Cylindrical Model; FEM: Finite Element Model, FLS: Finite Line Source; CSM: Cylinder Source Model; CaRM: Capacity Resistance Model.

Table A3. Pile and borehole case studies measuring both laboratory and field thermal conductivity.

| Reference | Hole Diameter   | Depth      | AR         | Ground Conditions                            | Lab Method                             | Field Method             | T <sub>injection</sub> > T <sub>ambient</sub> ? | Comments   |
|-----------|-----------------|------------|------------|--|--|--------------------------|---|--|
| [107]     | 0.15            | 100        | 658        | Clastic sedimentary sequence                 | Needle probe (93 measurements on core) | TRT, line-source         | Yes   | DTRT also carried out with higher resulting average effective thermal conductivity |
| [145]     | 0.136           | 86 to 99   | 632 to 728 | Shale, siltstone, and sandstone              | Needle probe (on dry cuttings)         | TRT, line source and FEA | Varies  | Four boreholes, varying test lengths including one long-term test                  |
| [176]     | >0.15           | 110 or 200 | >500       | Clay, silt, sand mudstone                    | Transient strip heat source            | TRT, line source         | ?   | 22 TRT on 11 boreholes, 337 samples tested   |
| [170]     | ?               | ?          | ?          | Sedimentary, volcanic, and metamorphic rocks | 1D transient source [244]              | TRT, line source         | ?   | 57 boreholes tested and laboratory results from 1398 rock cores                    |
| [177]     | 0.126           | 18.3       | 145        | Sand   | Needle probe                           | TRT, line source         | Yes   | Laboratory sand box  |
| [108]     | 0.25            | 30         | 120        | Sand and gravel with clay layers             | Needle probe                           | TRT, line source         | Varies  |  |
| [47]      | 0.3             | 26         | 87         | Stiff fissured clay                          | Needle probe                           | TRT, line source         | Yes   | Values from first stage of multi-stage TRT   |
| [152]     | 0.305 and 0.457 | 18.3       | 60 and 40  | Sandy clay and dense sand                    | Needle probe                           | TRT, line source         | Yes   |  |
| [174]     | 0.25            | 14.5       | 58         | Sand and gravel                              | Needle probe                           | TRT, line source and GPM | ?   | Short duration in situ test  |
| [175]     | 0.35            | 17.4       | 50         | Organic clay, sands, and gravels             | Needle and dual needle probes          | TRT, line source         | ?   | Square cross-section pile  |
| [163]     | 0.4             | 13.25      | 33         | Weathered granite                            | Needle probe                           | TRT, FEA                 | ?   | Spun concrete pile   |
| [172]     | 0.6             | 16.1       | 27         | Sand and clayey sand                         | Needle probe                           | TRT, line source         | Yes   |  |
| [173]     | 0.61            | 15.2       | 25         | Sand, sandstone                              | Needle probe                           | TRT, line source         | Yes   | Four piles, each test corrected for long header pipes                              |

TRT = thermal response test; FEA = finite element analysis.

## References

1. European Technology and Innovation Platform, Renewable Heating and Cooling. Geothermal Energy Panel. Available online: <http://www.rhc-platform.org/structure/geothermal-technology-panel/> (accessed on 6 July 2017).
2. Rees, S. *Advances in Ground Source Heat Pump Systems*; Woodhead Publishing: Sawston, UK, 2016; ISBN 978-0-08-100311-4.
3. Brandl, H. Energy foundations and other thermo-active ground structures. *Geotechnique* **2006**, *56*, 81–122. [[CrossRef](#)]
4. Adam, D.; Markiewicz, R. Energy from earth-coupled structures, foundations, tunnels and sewers. *Géotechnique* **2009**, *59*, 229–236. [[CrossRef](#)]
5. Bidarmaghaz, A.; Narsilio, G.; Johnston, I. Numerical Modelling of Ground Heat Exchangers with Different Ground Loop Configurations for Direct Geothermal Applications. In Proceedings of the 18th International Conference on Soil Mechanics and Geotechnical Engineering, Paris, France, 2–6 September 2013.
6. Batini, N.; Rotta Loira, A.F.; Conti, P.; Testi, D.; Grassie, W.; Laloui, L. Energy and geotechnical behaviour of energy piles for different design solutions. *Appl. Therm. Eng.* **2015**, *86*, 199–213. [[CrossRef](#)]
7. Alberti, L.; Angelotti, A.; Antelmi, M.; La Licata, I. A Numerical Study on the Impact of Grouting Material on Borehole Heat Exchangers Performance in Aquifers. *Energies* **2017**, *10*, 703. [[CrossRef](#)]
8. Delaleux, F.; Py, X.; Olives, R.; Dominguez, A. Enhancement of geothermal borehole heat exchangers performances by improvement of bentonite grouts conductivity. *Appl. Therm. Energy* **2012**, *33–34*, 92–99. [[CrossRef](#)]
9. Di Donna, A.; Barla, M. The role of ground conditions on energy tunnels' heat exchange. *Environ. Geotech.* **2016**, *3*, 214–224. [[CrossRef](#)]
10. Wołoszyn, J.; Gołas, A. Sensitivity analysis of efficiency thermal energy storage on selected rock mass and grout parameters using design of experiment method. *Energy Convers. Manag.* **2014**, *87*, 1297–1304. [[CrossRef](#)]
11. Low, J. Thermal Conductivity of Soils for Energy Foundation Applications. Ph.D. Thesis, University of Southampton, Southampton, UK, 2015.
12. Laloui, L.; Nuth, M.; Vulliet, L. Experimental and numerical investigations of the behaviour of heat exchanger pile. *Int. J. Numer. Anal. Methods Geomech.* **2006**, *30*, 763–781. [[CrossRef](#)]
13. Rees, S.; Adjali, M.; Zhou, Z.; Davies, M.; Thomas, H. Ground heat transfer effects on the thermal performance of earth-contact structures. *Renew. Sustain. Energy Rev.* **2000**, *4*, 213–265. [[CrossRef](#)]
14. Thirumaleshwar, M. *Fundamentals of Heat and Mass Transfer*; Pearson Education: Delhi, India, 2009; ISBN 8177585193.
15. De Vries, D.A. Simultaneous transfer of heat and moisture in porous media. *Trans. Am. Geophys. Union* **1958**, *39*, 909–916. [[CrossRef](#)]
16. De Vries, D.A. Thermal properties of soils. In *Physics of Plant Environment*, 2nd ed.; North-Holland Publishing Company: Amsterdam, The Netherlands, 1966.
17. De Vries, D.A. Heat transfer in soils. In *Heat and Mass Transfer in the Biosphere. Part 1. Transfer Processes in Plant Environment*; De Vries, D.A., Afghan, N.H., Eds.; John Wiley & Sons, Inc.: New York, NY, USA, 1974.
18. Woodside, W.; Messner, J.H. Thermal conductivity of porous media. I. Unconsolidated Sands. *J. Appl. Phys.* **1961**, *32*, 1688–1699. [[CrossRef](#)]
19. Farouki, O.T. *Thermal Properties of Soils*; No. CRREL-MONO-81-1; U.S. Army Corps of Engineers, Cold Regions Research and Engineering Laboratory: Hanover, NH, USA, 1981.
20. Midttømme, K.; Roaldset, E. Thermal conductivity of sedimentary rocks: Uncertainties in measurement and modelling. *Geol. Soc. Lond. Spec. Publ.* **1999**, *158*, 45–60. [[CrossRef](#)]
21. Hellstrom, G. *Ground Heat Storage, Thermal Analysis of Duct Storage Systems*; Department of Mathematical Physics, University of Lund: Lund, Sweden, 1991.
22. Liebel, H.T. Influence of Groundwater on Measurements of Thermal Properties in Fractured Aquifers. Ph.D. Thesis, Norwegian University of Science and Technology, Trondheim, Norway, 2012.
23. Campanella, R.G.; Mitchell, J.K. Influence of temperature variations on soil behavior. *J. Soil Mech. Found. Div.* **1968**.
24. Hueckel, T.; Baldi, G. Thermoplasticity of saturated clays: Experimental constitutive study. *J. Geotech. Eng. Div.* **1990**, *116*, 1778–1796. [[CrossRef](#)]

25. Cekerevac, C.; Laloui, L. Experimental study of the thermal effects on the mechanical behaviour of a clay. *Int. J. Numer. Anal. Methods Geomech.* **2004**, *28*, 209–228. [[CrossRef](#)]
26. Laloui, L.; Olgun, C.G.; Sutman, M.; McCartney, J.S.; Coccia, C.J.; Abuel-Naga, H.M.; Bowers, G.A. Issues involved with thermoactive geotechnical systems: Characterization of thermomechanical soil behavior and soil-structure interface behavior. *J. Deep Found. Inst.* **2014**, *8*, 108–112. [[CrossRef](#)]
27. Jensen, C.; Xing, C.; Folsom, C.; Ban, H.; Phillips, J. Design and validation of a high-temperature comparative thermal-conductivity measurement system. *Int. J. Thermophys.* **2012**, *33*, 311–329. [[CrossRef](#)]
28. ASTM International. *Standard Test Method for Steady-State Heat Flux Measurements and Thermal Transmission Properties by Means of the Guarded-Hot-Plate Apparatus*; ASTM C177–13; ASTM International: West Conshohocken, PA, USA, 2013. [[CrossRef](#)]
29. British Standards Institution (BSI). *Thermal Performance of Building Materials and Products. Determination of Thermal Resistance by Means of Guarded Hot Plate and Heat Flow Meter Methods. Products of High and Medium Thermal Resistance*; BS EN 12667:2001; British Standards Institution (BSI): London, UK, 2001.
30. International Organization for Standardization. *Thermal Insulation—Determination of Steady-State Thermal Resistance and Related Properties—Guarded Hot Plate Apparatus*; ISO 8302:1991; International Organization for Standardization: Geneva, Switzerland, 1991.
31. Salmon, D. Thermal conductivity of insulations using guarded hot plates, including recent developments and sources of reference materials. *Meas. Sci. Technol.* **2001**, *12*. [[CrossRef](#)]
32. Zhao, D.; Qian, X.; Gu, X.; Jajja, S.A.; Yang, R. Measurement Techniques for Thermal Conductivity and Interfacial Thermal Conductance of Bulk and Thin Film Materials. *J. Electron. Packag.* **2016**, *138*. [[CrossRef](#)]
33. Tarnawski, V.R.; Momose, T.; Leong, W.H.; Bovesecchi, G.; Coppa, P. Thermal conductivity of standard sands. Part I. Dry-state conditions. *Int. J. Thermophys.* **2009**, *30*, 949–968. [[CrossRef](#)]
34. Nikolaev, I.V.; Leong, W.H.; Rosen, M.A. Experimental investigation of soil thermal conductivity over a wide temperature range. *Int. J. Thermophys.* **2013**, *34*, 1110–1129. [[CrossRef](#)]
35. Hiraiwa, Y.; Kasubuchi, T. Temperature dependence of thermal conductivity over a wide range of temperature (5–75 °C). *Eur. J. Soil Sci.* **2000**, *51*, 211–218. [[CrossRef](#)]
36. Low, J.E.; Loveridge, F.A.; Powrie, W. Error analysis of the thermal cell for soil thermal conductivity measurement. In *Proceedings of the Institution of Civil Engineers ICE—Geotechnical Engineering*; ICE Publishing: London, UK, 2017; Volume 170, pp. 191–200. [[CrossRef](#)]
37. Clarke, B.G.; Agab, A.; Nicholson, D. Model specification to determine thermal conductivity of soils. In *Proceedings of the Institution of Civil Engineers—Geotechnical Engineering*; ICE publishing: London, UK, 2008; Volume 161, pp. 161–168. [[CrossRef](#)]
38. Alrtimi, A.; Rouainia, M.; Haigh, S. Thermal conductivity of a sandy soil. *Appl. Therm. Eng.* **2016**, *106*, 551–560. [[CrossRef](#)]
39. ASTM International. *Standard Test Method for Thermal Conductivity of Solids Using the Guarded-Comparative-Longitudinal Heat Flow Technique*; ASTM E1225-13; ASTM International: West Conshohocken, PA, USA, 2013. [[CrossRef](#)]
40. Barry-Macaulay, D.; Bouazza, A.; Singh, R.M.; Wang, B.; Ranjith, P.G. Thermal conductivity of soils and rocks from the Melbourne (Australia) region. *Eng. Geol.* **2013**, *164*, 131–138. [[CrossRef](#)]
41. Schmidt, A.J.; Cheaito, R.; Chiesa, M. A frequency-domain thermoreflectance method for the characterization of thermal properties. *Rev. Sci. Instrum.* **2009**, *80*, 094901. [[CrossRef](#)] [[PubMed](#)]
42. Van der Held, E.F.M.; Van Drunen, F.G. A method of measuring the thermal conductivity of liquids. *Physica* **1949**, *15*, 865–881. [[CrossRef](#)]
43. Blackwell, J.H. A transient-flow method for determination of thermal constants of insulating materials in bulk Part I—Theory. *J. Appl. Phys.* **1954**, *25*, 137–144. [[CrossRef](#)]
44. Teka, Thermophysical Instruments-Geothermal Investigation. 2017. Available online: <http://www.te-ka.de/index.php/en/> (accessed on 6 July 2017).
45. Isomet. Portable Heat Transfer Analyser. Available online: <http://appliedp.com/produkty/isomet/> (accessed on 29 November 2017).
46. ASTM International. *Standard Test Method for Determination of Thermal Conductivity of Soil and Soft Rock by Thermal Needle Probe Procedure*; ASTM D5334–14; ASTM International: West Conshohocken, PA, USA, 2000. [[CrossRef](#)]

47. Low, J.; Loveridge, F.; Powrie, W. A comparison of laboratory and in situ methods to determine soil thermal conductivity for energy foundations and other ground heat exchanger applications. *Acta Geotech.* **2015**, *10*, 209–218. [[CrossRef](#)]
48. Kasubuchi, T. Development of in-situ soil water measurement by heat-probe method. *Jpn. Agric. Res. Q.* **1992**, *26*, 178–181.
49. Campbell, G.S.; Calissendorff, C.; Williams, J.H. Probe for measuring soil specific heat using a heat-pulse method. *Soil Sci. Soc. Am. J.* **1991**, *55*, 291–293. [[CrossRef](#)]
50. Bilskie, J.R. Dual Probe Methods for Determining Soil Thermal Properties: Numerical Laboratory Study. Ph.D. Thesis, Iowa State University, Ames, IA, USA, 1994.
51. Rajeev, P.; Kodikara, J. Estimating apparent thermal diffusivity of soil using field temperature time series. *Geomech. Geoengin.* **2016**, *11*, 28–46. [[CrossRef](#)]
52. Lockmuller, N.; Redgrove, J.; Kubicar, L.U. Measurement of thermal conductivity with the needle probe. *High Temp. High Press.* **2003**, *35*, 127–138. [[CrossRef](#)]
53. Valente, A.; Morais, R.; Tuli, A.; Hopmans, J.W.; Kluitenberg, G.J. Multi-functional probe for small-scale simultaneous measurements of soil thermal properties, water content, and electrical conductivity. *Sens. Actuators* **2006**, *132*, 70–77. [[CrossRef](#)]
54. Assael, M.J.; Antoniadis, K.D.; Wakeham, W.A. Historical evolution of the transient hot-wire technique. *Int. J. Thermophys.* **2010**, *31*, 1051–1072. [[CrossRef](#)]
55. Merckx, B.; Dudoignon, P.; Garnier, J.P.; Marchand, D. Simplified transient hot-wire method for effective thermal conductivity measurement in geo materials: Microstructure and saturation effect. *Adv. Civ. Eng.* **2012**, *2012*. [[CrossRef](#)]
56. International Organization for Standardization. *Plastics—Determination of Thermal Conductivity and Thermal Diffusivity—Part 2: Transient Plane Heat Source (Hot Disc) Method*; ISO 22007-2:2015; International Organization for Standardization: Geneva, Switzerland, 2015.
57. Gustafsson, S.; Thermetrol, A.B. Device for Measuring Thermal Properties of a Test Substance—the Transient Plane Source (TPS) Method. U.S. Patent 5,044,767, 1991.
58. Gustafsson, S.E. Transient plane source techniques for thermal conductivity and thermal diffusivity measurements of solid materials. *Rev. Sci. Instrum.* **1991**, *62*, 797–804. [[CrossRef](#)]
59. Mikulić, D.; Milovanović, B. TCi System for Non-Destructive Determination of Thermal Properties of Materials. In Proceedings of the 10th European Conference on Non-Destructive Testing, Moscow, Russia, 7–11 June 2010; ICNDT: Northampton, UK, 2010; pp. 1364–1373.
60. Thermtest Inc. Thermtest Thermophysical Instruments. Available online: <https://thermtest.com/tps-global> (accessed on 6 July 2017).
61. C-Therm Technologies Ltd. TCi Thermal Conductivity Analyzer. Available online: [http://ctherm.com/products/tci\\_thermal\\_conductivity/](http://ctherm.com/products/tci_thermal_conductivity/) (accessed on 6 July 2017).
62. Suleiman, B.M. Thermal Conductivity of Saturated samples using the Hot-Disk Technique. In Proceedings of the 4th WSEAS International Conference on Heat Transfer, Thermal Engineering and Environment, Elounda, Greece, 21–23 August 2006.
63. Florides, G.; Theofanous, E.; Iosif-Stylianou, I.; Tassou, S.; Christodoulides, P.; Zomeni, Z.; Tsiolakis, E.; Kalogirou, S.; Messaritis, V.; Pouloupatis, P.; et al. Modeling and assessment of the efficiency of horizontal and vertical ground heat exchangers. *Energy* **2013**, *58*, 655–663. [[CrossRef](#)]
64. Stylianou, I.I.; Tassou, S.; Christodoulides, P.; Panayides, I.; Florides, G. Measurement and analysis of thermal properties of rocks for the compilation of geothermal maps of Cyprus. *Renew. Energy* **2016**, *88*, 418–429. [[CrossRef](#)]
65. Stylianou, I.I.; Florides, G.; Tassou, S.; Tsiolakis, E.; Christodoulides, P. Methodology for estimating the ground heat absorption rate of Ground Heat Exchangers. *Energy* **2017**, *127*, 258–270. [[CrossRef](#)]
66. Popov, Y.A.; Pribnow, D.F.C.; Sass, J.H.; Williams, C.F.; Burkhardt, H. Characterization of rock thermal conductivity by high-resolution optical scanning. *Geothermics* **1999**, *28*, 253–276. [[CrossRef](#)]
67. Haffen, S.; Geraud, Y.; Diraison, M.; Dezayes, C. Determining fluid flow zones in a geothermal reservoir from thermal conductivity and temperature. *Geothermics* **2013**, *46*, 32–41. [[CrossRef](#)]
68. Liu, S.; Feng, C.; Wang, L.; Li, C. Measurement and analysis of thermal conductivity of rocks in the Tarim Basin, Northwest China. *Acta Geol. Sin. (Engl. Ed.)* **2011**, *85*, 598–609. [[CrossRef](#)]

69. Mitchell, J.K.; Kao, T.C. Measurement of soil thermal resistivity. *J. Geotech. Geoenviron. Eng.* **1978**, *104*, 1307–1320.
70. Slusarchuk, W.A.; Foulger, P.H. *Development and Calibration of a Thermal Conductivity Probe Apparatus for Use in the Field and Laboratory*. National Research Council of Canada, Division of Building Research; Technical Paper No. 388; National Research Council Canada: Ottawa, ON, Canada, 1973.
71. Tarnawski, V.R.; Momose, T.; Leong, W.H. Thermal conductivity of standard sands II. Saturated conditions. *Int. J. Thermophys.* **2011**, *32*, 984–1005. [[CrossRef](#)]
72. Tarnawski, V.R.; McCombie, M.L.; Momose, T.; Sakaguchi, I.; Leong, W.H. Thermal conductivity of standard sands. Part III. Full range of saturation. *Int. J. Thermophys.* **2013**, *34*, 1130–1147. [[CrossRef](#)]
73. Woodside, W.; Cliffe, J.B. Heat and moisture transfer in closed systems of two granular materials. *Soil Sci.* **1959**, *87*, 75–82. [[CrossRef](#)]
74. Kersten, M.S. *Thermal Properties of Soils*; Bulletin 28; University of Minnesota, Institute of Technology, Engineering Experiment Station: Minneapolis, MN, USA, 1949; Volume LII.
75. Jackson, R.D.; Taylor, S.A. Thermal conductivity and diffusivity. In *Methods of Soil Analysis: Part 1—Physical and Mineralogical Methods*; Klute, A., Ed.; Soil Science Society of America, American Society of Agronomy: Madison, WI, USA, 1986.
76. Sass, J.H.; Lachenbruch, A.H.; Munroe, R.J. Thermal conductivity of rocks from measurements on fragments and its application to heat-flow determinations. *J. Geophys. Res.* **1971**, *76*, 3391–3401. [[CrossRef](#)]
77. Moench, A.F.; Evans, D.D. Thermal conductivity and diffusivity of soil using a cylindrical heat source. *Soil Sci. Soc. Am. J.* **1970**, *34*, 377–381. [[CrossRef](#)]
78. Bligh, T.P.; Smith, E.A. Thermal conductivity measurements of soils in the field and laboratory using a thermal conductivity probe. *Energy Effic. Build. Syst. Rep.* **1983**, *25*, 275.
79. Jorand, R.; Vogt, C.; Marquart, G.; Clauser, C. Effective thermal conductivity of heterogeneous rocks from laboratory experiments and numerical modelling. *J. Geophys. Res. Solid Earth* **2013**, *118*, 5225–5235. [[CrossRef](#)]
80. Smits, K.M.; Sakaki, T.; Limsuwat, A.; Illangasekare, T.H. Thermal conductivity of sands under varying moisture and porosity in drainage–wetting cycles. *Vadose Zone J.* **2010**, *9*, 172–180. [[CrossRef](#)]
81. Johansen, O. *Thermal Conductivity of Soils*; Draft Translated: 637; U.S. Army Corps of Engineering, Cold Regions Research and Engineering Laboratory: Hanover, NH, USA, 1977.
82. Côté, J.; Konrad, J.M. A generalized thermal conductivity model for soils and construction materials. *Can. Geotech. J.* **2005**, *42*, 443–458. [[CrossRef](#)]
83. Côté, J.; Konrad, J.M. Assessment of structure effects on the thermal conductivity of two-phase porous geomaterials. *Int. J. Heat Mass Trans.* **2009**, *52*, 796–804. [[CrossRef](#)]
84. Antilén, M.; Escudey, M.; Förster, J.E.; Moraga, N.; Marty, D.; Fudym, O. Application of the hot disk method to the thermophysical characterization of soils. *J. Chil. Chem. Soc.* **2003**, *48*, 27–29. [[CrossRef](#)]
85. Mogensen, P. Fluid to Duct Wall Heat Transfer in Duct System Heat Storage. In Proceedings of the International Conference on Subsurface Heat Storage in Theory and Practice, Stockholm, Sweden, 6–8 June 1983; Swedish Council for Building Research: Stockholm, Sweden, 1983; pp. 652–657.
86. Gehlin, S. Thermal Response Test: Method Development and Evaluation. Ph.D. Thesis, Luleå University of Technology, Luleå, Sweden, 2002.
87. VDI-Standards. VDI 4640 blatt 3 utilization of the subsurface for thermal purposes. In *Underground Thermal Energy Storage*; VDI-Gesellschaft Energie und Umwelt (GEU): Berlin, Germany, 2001.
88. Spitler, J.D.; Gehlin, S.E.A. Thermal response testing for ground source heat pump systems—An historical review. *Renew. Sustain. Energy Rev.* **2015**, *50*, 1125–1137. [[CrossRef](#)]
89. Witte, H.J.L. In situ estimation of ground thermal properties. In *Advances in Ground-Source Heat Pump Systems*; Rees, S., Ed.; Woodhead Publishing: Sawston, UK, 2016.
90. Zhang, C.; Guo, Z.; Liu, Y.; Cong, X.; Peng, D. A review on thermal response test of ground-coupled heat pump systems. *Renew. Sustain. Energy Rev.* **2014**, *40*, 851–867. [[CrossRef](#)]
91. Li, M.; Lai, A.C. Review of analytical models for heat transfer by vertical ground heat exchangers (GHEs): A perspective of time and space scales. *Appl. Energy* **2015**, *151*, 178–191. [[CrossRef](#)]
92. Microgeneration Installation Standard. *MIS 3005 Microgeneration Installation Standard: Requirements for MCS Contractors Undertaking the Supply, Design, Installation, Set to Work, Commissioning and Handover of Microgeneration Heat Pump Systems, Issue 4.3*; Microgeneration Installation Standard, Department of Energy and Climate Change: London, UK, 2008.



93. Recknagel, H.; Sprenger, E.; Schramek, E.-R. *Génie Climatique [Taschenbuch für Heizung und Klimatechnik]*; Bodson, A., Caradec, C., Pastureau, S., Petit, N., Eds.; Clima & Confort: Dunod, Paris, France, 2013.
94. Javed, S. Design of ground source heat pump systems. Thermal Modelling and Evaluation of Borehole Heat Transfer. Ph.D. Thesis, Chalmers University of Technology, Göteborg, Sweden, 2012.
95. Kavanaugh, S.P.; Rafferty, K.D.; American Society of Heating, Refrigerating and Air-Conditioning Engineers (ASHRAE). *Ground-Source Heat Pumps: Design of Geothermal Systems for Commercial and Institutional Buildings*; American Society of Heating, Refrigerating and Air-Conditioning Engineers: Atlanta, GA, USA, 1997.
96. Kurevija, T.; Vulin, D.; Macenić, M. Impact of geothermal gradient on ground source heat pump system modeling. *Rud. Geol. Naft. Zb.* **2014**, *28*, 39–45.
97. Dehkordi, S.E.; Schincariol, R.A. Effect of thermal-hydrogeological and borehole heat exchanger properties on performance and impact of vertical closed-loop geothermal heat pump systems. *Hydrogeol. J.* **2014**, *22*, 189–203. [[CrossRef](#)]
98. Radioti, G.; Sartor, K.; Charlier, R.; Dewallef, P.; Nguyen, F. Effect of undisturbed ground temperature on the design of closed-loop geothermal systems: A case study in a semi-urban environment. *Appl. Energy* **2017**, *200*, 89–105. [[CrossRef](#)]
99. Kavanaugh, S.P.; Xie, L.; Martin, C. TRP-1118—Investigation of Methods for Determining Soil and Rock Formation Thermal Properties from Short Term Field Test; Final Report; American Society of Heating, Refrigerating and Air-Conditioning Engineers (ASHRAE): Atlanta, GA, USA, 2000.
100. Javed, S.; Fahlén, P. Thermal response testing of a multiple borehole ground heat exchanger. *Int. J. Low-Carbon Technol.* **2011**, *6*, 141–148. [[CrossRef](#)]
101. Gehlin, S.; Nordell, B. Determining undisturbed ground temperature for thermal response test. *ASHRAE Trans.* **2003**, *109*, 151–156.
102. Taniguchi, M.; Uemura, T. Effects of urbanization and groundwater flow on the subsurface temperature in Osaka, Japan. *Phys. Earth Planet. Inter.* **2005**, *152*, 305–313. [[CrossRef](#)]
103. Banks, D. *An Introduction to Thermogeology. Ground Source Heating and Cooling*; Blackwell Publishing: Oxford, UK, 2008; ISBN 978-0-470-67034-7.
104. Ferguson, G.; Woodbury, A.D. Urban heat island in the subsurface. *Geophys. Res. Lett.* **2007**, *34*. [[CrossRef](#)]
105. Zhu, K.; Blum, P.; Ferguson, G.; Balke, K.D.; Bayer, P. The geothermal potential of urban heat islands. *Environ. Res. Lett.* **2010**, *5*. [[CrossRef](#)]
106. Menberg, K.; Bayer, P.; Zosseder, K.; Rumohr, S.; Blum, P. Subsurface urban heat islands in German cities. *Sci. Total Environ.* **2013**, *442*, 123–133. [[CrossRef](#)] [[PubMed](#)]
107. Soldo, V.; Borović, S.; Lepoša, L.; Boban, L. Comparison of different methods for ground thermal properties determination in a clastic sedimentary environment. *Geothermics* **2016**, *61*, 1–11. [[CrossRef](#)]
108. Witte, H.J.L.; van Gelder, G.J.; Spitler, J.D. In Situ Measurement of Ground Thermal Conductivity: A Dutch Perspective. *ASHRAE Trans.* **2002**, *108*, 263–272.
109. Wang, H.; Qi, C.; Du, H.; Gu, J. Improved method and case study of thermal response test for borehole heat exchangers of ground source heat pump system. *Renew. Energy* **2010**, *35*, 727–733. [[CrossRef](#)]
110. Javed, S.; Nakos, H.; Claesson, J. A method to evaluate thermal response tests on groundwater-filled boreholes. *ASHRAE Trans.* **2012**, *118*, 540–549.
111. Acuña, J.; Palm, B. Distributed thermal response tests on pipe-in-pipe borehole heat exchangers. *Appl. Energy* **2013**, *109*, 312–320. [[CrossRef](#)]
112. Raymond, J.; Lamarche, L. Development and numerical validation of a novel thermal response test with a low power source. *Geothermics* **2014**, *51*, 434–444. [[CrossRef](#)]
113. Dornstädter, J.; Heidinger, P.; Heinemann-Glutsch, B. Erfahrungen aus der Praxis mit dem Enhanced Geothermal Response Test (EGRT). In Proceedings of the Der Geothermiekongress 2008, Karlsruhe, Germany, 11–13 November 2008; pp. 271–279.
114. Poulsen, S.E.; Alberdi-Pagola, M. Interpretation of ongoing thermal response tests of vertical (BHE) borehole heat exchangers with predictive uncertainty based stopping criterion. *Energy* **2015**, *88*, 157–167. [[CrossRef](#)]
115. Ingersoll, L.R.; Zobel, O.J.; Ingersoll, A.C. *Heat Conduction with Engineering, Geological, and Other Applications*; The University of Wisconsin Press: Madison, WI, USA, 1954.
116. Carslaw, H.S.; Jaeger, J.C. *Conduction of Heat in Solids*; Clarendon Press: Oxford, UK, 1959; ISBN 0-19-853368-3.



117. American Society of Heating, Refrigerating and Air-Conditioning Engineer (ASHRAE). *2007 ASHRAE Handbook—Heating, Ventilating, and Air-Conditioning Applications (I-P Edition)*; American Society of Heating, Refrigerating and Air-Conditioning Engineers, Inc.: Atlanta, GA, USA, 2007.
118. Beier, R.A.; Smith, M.D. Minimum duration of in-situ tests on vertical boreholes. *ASHRAE Trans.* **2003**, *109*, 475–486.
119. Shonder, J.A.; Beck, J. *A New Method to Determine the Thermal Properties of Soil Formations From in Situ Field Tests*; Report ORNL/TM-2000/97; Oak Ridge National Laboratory: Oak Ridge, TN, USA, 2000.
120. Austin, W.; Yavuzturk, C.; Spitler, J.D. Development of an In-Situ System and Analysis Procedure for Measuring Ground Thermal Properties. *ASHRAE Trans.* **2000**, *106*, 365–379.
121. Nakos, H. Response Testing and Evaluation of Groundwater-Filled Boreholes: Development and Validation of a New Calculation Tool. Master's Thesis, Chalmers University of Technology, Göteborg, Sweden, 2011.
122. Javed, S.; Claesson, J. New analytical and numerical solutions for the short-term analysis of vertical ground heat exchangers. *ASHRAE Trans.* **2011**, *117*, 3–12.
123. Marcotte, D.; Pasquier, P. On the estimation of thermal resistance in borehole thermal conductivity test. *Renew. Energy* **2008**, *33*, 2407–2415. [[CrossRef](#)]
124. Javed, S.; Spitler, J.; Fahlén, P. An experimental investigation of the accuracy of thermal response tests used to measure ground thermal properties. *ASHRAE Trans.* **2011**, *117*, 13–21.
125. Javed, S.; Spitler, J. Accuracy of borehole thermal resistance calculation methods for grouted single U-tube ground heat exchangers. *Appl. Energy* **2017**, *187*, 790–806. [[CrossRef](#)]
126. Lamarche, L.; Kaji, S.; Beauchamp, B. A review of methods to evaluate borehole thermal resistances in geothermal heat-pump systems. *Geothermics* **2010**, *39*, 187–200. [[CrossRef](#)]
127. Spitler, J.D.; Javed, S.; Ramstad, R.K. Natural convection in groundwater-filled boreholes used as ground heat exchangers. *Appl. Energy* **2016**, *164*, 352–365. [[CrossRef](#)]
128. Witte, H.J.L. Error analysis of thermal response tests. *Appl. Energy* **2013**, *109*, 302–311. [[CrossRef](#)]
129. Javed, S. Thermal response testing: Results and experiences from a ground source heat pump test facility with multiple boreholes. In Proceedings of the 11th REHVA World Congress (Clima 2013), Prague, Czech Republic, 16–19 June 2013.
130. Bandos, T.V.; Montero, Á.; Córdoba, P.F.D.; Urchueguía, J.F. Improving parameter estimates obtained from thermal response tests: Effect of ambient air temperature variations. *Geothermics* **2011**, *40*, 136–143. [[CrossRef](#)]
131. Sanner, B.; Mands, E.; Sauer, M.; Grundmann, E. Technology, development status, and routine application of Thermal Response Test. In Proceedings of the European Geothermal Congress 2007, Unterhaching, Germany, 30 May–1 June 2007.
132. Diao, N.; Li, Q.; Fang, Z. Heat transfer in ground heat exchangers with groundwater advection. *Int. J. Therm. Sci.* **2004**, *43*, 1203–1211. [[CrossRef](#)]
133. Raymond, J.; Therrien, R.; Gosselin, L.; Lefebvre, R. Numerical analysis of thermal response tests with a groundwater flow and heat transfer model. *Renew. Energy* **2011**, *36*, 315–324. [[CrossRef](#)]
134. Wagner, V.; Blum, P.; Kübert, M.; Bayer, P. Analytical approach to groundwater-influenced thermal response tests of grouted borehole heat exchangers. *Geothermics* **2013**, *46*, 22–31. [[CrossRef](#)]
135. Verdoya, M.; Chiozzi, P. Influence of groundwater flow on the estimation of subsurface thermal parameters. *Int. J. Earth Sci.* **2016**, 1–8. [[CrossRef](#)]
136. Beier, R.A.; Smith, M.D. Removing Variable Heat Rate Effects from Borehole Tests. *ASHRAE Trans.* **2003**, *109*, 463–474.
137. Sauer, M. Evaluating improper response test data by using superposition of line source approximation. In Proceedings of the European Geothermal Congress EGC 2013, Pisa, Italy, 3–8 June 2013.
138. Hu, P.; Meng, Q.; Sun, Q.; Zhu, N.; Guan, C. A method and case study of thermal response test with unstable heat rate. *Energy Build.* **2012**, *48*, 199–205. [[CrossRef](#)]
139. Spitler, J.; Rees, S.; Yavuzturk, C. *More Comments on In-Situ Borehole Thermal Conductivity Testing*; The Source: Barrie, ON, Canada, 1999; Volume 12, pp. 4–6.
140. Gehlin, S.; Hellstrom, G. Influence on thermal response test by groundwater flow in vertical fractures in hard rock. *Renew. Energy* **2003**, *28*, 2221–2238. [[CrossRef](#)]
141. Fujii, H.; Hiroaki, O.; Itoi, R. Thermal Response Tests Using Optical Fiber Thermometers. *GRC Trans.* **2006**, *30*, 545–551.

142. Florides, G.; Kalogirou, S. First in situ determination of the thermal performance of a U-pipe borehole heat exchanger, in Cyprus. *Appl. Therm. Eng.* **2008**, *28*, 157–163. [[CrossRef](#)]
143. Acuña, J.; Mogensen, P.; Palm, B. Distributed thermal response test on a U-pipe borehole heat exchanger. In Proceedings of the 11th International Conference on Thermal Energy Storage Effstock 2009, Stockholm, Sweden, 14–17 June 2009; Academic Conferences Publishing: Stockholm, Sweden, 2009.
144. Loveridge, F.; Holmes, G.; Powrie, W.; Roberts, T. Thermal response testing through the chalk aquifer. In *Proceedings of the Institution of Civil Engineers ICE—Geotechnical Engineering*; ICE publishing: London, UK, 2013; Volume 166, pp. 197–210. [[CrossRef](#)]
145. Radioti, G.; Delvoie, S.; Charlier, R.; Dumont, G.; Nguyen, F. Heterogeneous bedrock investigation for a closed-loop geothermal system: A case study. *Geothermics* **2016**, *62*, 79–92. [[CrossRef](#)]
146. Heske, C.; Kohlsch, O.; Dornstädter, J.; Heidinger, P. Der Enhanced-Geothermal-Response Test als Auslegungsgrundlage und Optimierungstool. *Geothermische Standorterkundung: Sonderheft Oberflächennahe Geothermie. Bbr Fachmagazin für Brunnen- und Leitungsbau* **2011**, *62*, 36–43. (In German)
147. Liebel, H.T.; Huber, K.; Frengstad, B.S.; Ramstad, R.K.; Brattli, B. Temperature footprint of a thermal response test can help to reveal thermogeological information. *Nor. Geol Unders. Bull.* **2011**, *451*, 20–31.
148. Fujii, H.; Okubo, H.; Nishi, K.; Itoi, R.; Ohyama, K.; Shibata, K. An improved thermal response test for U-tube ground heat exchanger based on optical fiber thermometers. *Geothermics* **2009**, *38*, 399–406. [[CrossRef](#)]
149. Hausner, M.B.; Suarez, F.; Glander, K.E.; Van De Giesen, N.; Selker, J.S.; Tyler, S.W. Calibrating single-ended fiber-optic raman spectra distributed temperature sensing data. *Sensors* **2011**, *11*, 10859–10879. [[CrossRef](#)] [[PubMed](#)]
150. Raymond, J.; Lamarche, L. Simulation of thermal response tests in a layered subsurface. *Appl. Energy* **2013**, *109*, 293–301. [[CrossRef](#)]
151. Brandl, H. Thermo-active Ground-Source Structures for Heating and Cooling. *Procedia Eng.* **2013**, *57*, 9–18. [[CrossRef](#)]
152. Loveridge, F.; Brettmann, T.; Olgun, G.; Powrie, W. Assessing the applicability of thermal response testing to energy piles. In Proceedings of the Global Perspectives on the sustainable Execution of Foundations Works, Stockholm, Sweden, 21–23 May 2014.
153. GSHP Association. *Thermal Pile: Design, Installation & Materials Standards*; Ground Source Heat Pump Association National Energy Centre: Milton Keynes, UK, 2012; p. 85.
154. Loveridge, F.; Powrie, W. Temperature response functions (G-functions) for single pile heat exchangers. *Energy* **2013**, *57*, 554–564. [[CrossRef](#)]
155. Claesson, J.; Javed, S. An analytical method to calculate borehole fluid temperatures for time-scales from minutes to decades. *ASHRAE Trans.* **2011**, *117*, 279–288.
156. Bandos, T.V.; Campos-Celador, Á.; López-González, L.M.; Sala-Lizarraga, J.M. Finite cylinder-source model for energy pile heat exchangers: Effects of thermal storage and vertical temperature variations. *Energy* **2014**, *78*, 639–648. [[CrossRef](#)]
157. Hu, P.; Zha, J.; Lei, F.; Zhu, N.; Wu, T. A composite cylindrical model and its application in analysis of thermal response and performance for energy pile. *Energy Build.* **2014**, *84*, 324–332. [[CrossRef](#)]
158. Man, Y.; Yang, H.; Diao, N.; Liu, J.; Fang, Z. A new model and analytical solutions for borehole and pile ground heat exchangers. *Int. J. Heat Mass Transfer* **2010**, *53*, 2593–2601. [[CrossRef](#)]
159. Maragna, C.; Rachez, X. Innovative Methodology to Compute the Temperature Evolution of Pile Heat Exchangers. In Proceedings of the World Geothermal Congress, Melbourne, Australia, 19–25 April 2015.
160. Zarrella, A.; Emmi, G.; Zecchin, R.; de Carli, M. An appropriate use of the thermal response test for the design of energy foundation piles with U-tube circuits. *Energy Build.* **2017**, *134*, 259–270. [[CrossRef](#)]
161. De Carli, M.; Tonon, M.; Zarrella, A.; Zecchin, R. A computational capacity resistance model (CaRM) for vertical ground-coupled heat exchangers. *Renew. Energy* **2010**, *35*, 1537–1550. [[CrossRef](#)]
162. Franco, A.; Moffat, R.; Toledo, M.; Herrera, P. Numerical sensitivity analysis of thermal response tests (TRT) in energy piles. *Renew. Energy* **2016**, *86*, 985–992. [[CrossRef](#)]
163. Park, H.; Lee, S.R.; Yoon, S.; Choi, J.C. Evaluation of thermal response and performance of PHC energy pile: Field experiments and numerical simulation. *Appl. Energy* **2013**, *103*, 12–24. [[CrossRef](#)]

164. Cecinato, F.; Loveridge, F.A.; Gajo, A.; Powrie, W. A new modelling approach for piled and other ground heat exchanger applications. In Proceedings of the XVI European Conference on Soil Mechanics and Geotechnical Engineering 2015, Edinburgh, UK, 13–17 September 2015; ICE Institution of Civil Engineers: London, UK, 2015.
165. Cecinato, F.; Loveridge, F.A. Influences on the thermal efficiency of energy piles. *Energy* **2015**, *82*, 1021–1033. [[CrossRef](#)]
166. Loveridge, F.; Powrie, W.; Nicholson, D. Comparison of two different models for pile thermal response test interpretation. *Acta Geotech.* **2014**, *9*, 367–384. [[CrossRef](#)]
167. Ozudogru, T.; Brettmann, T.; Guney Olgun, C.; Martin, I.J.; Senol, A. Thermal Conductivity Testing of Energy Piles: Field Testing and Numerical Modeling. In Proceedings of the GeoCongress 2012, State of the Art and Practice in Geotechnical Engineering, Oakland, CA, USA, 25–29 March 2012.
168. Alberdi-Pagola, M.; Poulsen, S.E. Thermal response testing and performance of quadratic cross section energy piles (Vejle, Denmark). In Proceedings of the XVI European Conference on Soil Mechanics and Geotechnical Engineering 2015, Edinburgh, UK, 13–17 September 2015; ICE Institution of Civil Engineers: London, UK, 2015.
169. Schulze-Makuch, D.; Carlson, D.A.; Cherkauer, D.S.; Malik, P. Scale Dependency of Hydraulic Conductivity in Heterogeneous Media. *Water* **1999**, *37*, 904–919. [[CrossRef](#)]
170. Liebel, H.T.; Huber, K.; Frengstad, B.S.; Kalskin Ramstad, R.; Brattli, B. Rock core samples cannot replace thermal response tests—A statistical comparison based on thermal conductivity data from the Oslo Region (Norway). In *Zero Emission Buildings, Proceedings of the Renewable Energy 682 Research Conference, Trondheim, Norway, 7–8 June 2010*; Haase, M., Hestnes, A.G., Eds.; Renewable Energy Conference & Tapir Academic Press: Trondheim, Norway, 2010; pp. 145–154.
171. Radioti, G. Shallow Geothermal Energy: Effect of In Situ Conditions on Borehole Heat Exchanger Design and Performance. Ph.D. Thesis, University of Liège, Liège, Belgium, 2016.
172. Bouazza, A.; Wang, B.; Singh, R.M. Soil effective thermal conductivity from energy pile thermal tests. In *Coupled Phenomena in Environmental Geotechnics, Proceedings of the International Symposium, Torino, Italy, 1–3 July 2013*; Taylor & Francis: London, UK, 2013; pp. 211–219.
173. Murphy, K.D.; McCartney, J.S.; Henry, K.S. Impact of horizontal run-out length on the thermal response of full-scale energy foundations. In *Geo-Congress 2014 Technical Papers: Geo-Characterization and Modeling for Sustainability*; ASCE: Reston, VA, USA, 2014; pp. 2715–2724.
174. Hemmingway, P.; Long, M. Energy piles: Site investigation and analysis. In *Proceedings of the Institution of Civil Engineers—Geotechnical Engineering*; ICE publishing: London, UK, 2013; Volume 166, pp. 561–575.
175. Badenes, B.; de Santiago, C.; Nope, F.; Magraner, T.; Urchueguia, J.; de Groot, M.; Pardo de Santayana, F.; Arcos, J.L.; Martin, F. Thermal characterization of a geothermal precast pile in Valencia (Spain). In Proceedings of the European Geothermal Congress 2016, Strasbourg, France, 19–24 September 2016.
176. Zhang, Y.; Gao, P.; Yu, Z.; Fang, J.; Li, C. Characteristics of ground thermal properties in Harbin, China. *Energy Build.* **2014**, *69*, 51–259. [[CrossRef](#)]
177. Beier, R.A.; Smith, M.D.; Spitler, J.D. Reference data sets for vertical boreholes ground heat exchanger models and thermal response tests analysis. *Geothermics* **2011**, *40*, 79–85. [[CrossRef](#)]
178. Graham, J. The 2003 R.M. Hardy Lecture: Soil parameters for numerical analysis in clay. *Can. Geotech. J.* **2006**, *43*, 187–209. [[CrossRef](#)]
179. Dong, Y.; McCartney, J.S.; Lu, N. Critical review of thermal conductivity models for unsaturated soils. *Geotech. Geol. Eng.* **2015**, *33*, 207–221.
180. Allani, M.; Van Lysebetten, G.; Huybrechts, N. Experimental and numerical study of the thermo-mechanical behaviour of energy piles for Belgian practice. In *Advances in Laboratory Testing and Modelling of Soils and Shales (ATMSS)*, 1st ed.; Ferrari, A., Laloui, L., Eds.; Springer International Publishing: Cham, Switzerland, 2017; pp. 405–412, ISBN 978-3-319-52773-4.
181. Sanner, B. Overview of shallow geothermal systems. In *Geotrained Training Manual for Designers of Shallow Geothermal Systems*; McCorry, M., Jones, G.L.L., Eds.; European Federation of Geologists: Brussels, Belgium, 2011; pp. 7–14.
182. Morpher-Busch, L. Instructions for Using the Thermomap Viewer. 2013. Available online: [http://geoweb2.sbg.ac.at/thermomap/Instruction\\_Manual\\_Map\\_Viewer.pdf](http://geoweb2.sbg.ac.at/thermomap/Instruction_Manual_Map_Viewer.pdf) (accessed on 20 February 2017).

183. C rmak, V.; Rybach, L. Thermal conductivity and specific heat of minerals and rock. In *Geophysics—Physical Properties of Rocks, Landolt-Bornstein Numerical Data and Functional Relationships in Science and Technology*; New Series, Group V; Springer: Berlin, Germany, 1982; pp. 305–343.
184. Yavari, N.; Tang, M.; Pereira, J.M.; Hassen, G. Effect of temperature on the shear strength of soils and the soil–structure interface. *Can. Geotech. J.* **2016**, *53*, 1186–1194. [[CrossRef](#)]
185. Eriksson, L. Temperature effects on consolidation properties of sulphide clays. In *Proceedings of the 12th International Conference on Soil Mechanics and Foundation Engineering*, Rio de Janeiro, Brazil, 13–18 August 1989; Taylor & Francis: Rotterdam, The Netherlands, 1989.
186. Leroueil, S.; Marques, M.E.S. Importance of strain rate and temperature effects in geotechnical engineering. In *Measuring and Modelling Time Dependent Soil Behaviour*; Geotechnical Special Publication (Book 61); Sheahan, T.C., Kaliakin, V.N., Eds.; American Society of Civil Engineers: New York, NY, USA, 1996.
187. Vardoulakis, I. Dynamic thermo-poro-mechanical analysis of catastrophic landslides. *G otechnique* **2002**, *52*, 151–171. [[CrossRef](#)]
188. Cecinato, F.; Zervos, A.; Veveakis, E. A thermomechanical model for the catastrophic collapse of large landslides. *Int. J. Numer. Anal. Methods Geomech.* **2011**, *35*, 1507–1535. [[CrossRef](#)]
189. Cecinato, F.; Zervos, A. Influence of thermomechanics in the catastrophic collapse of planar landslides. *Can. Geotech. J.* **2012**, *49*, 207–225. [[CrossRef](#)]
190. Alonso, E.E.; Zervos, A.; Pinyol, N.M. Thermo-poro-mechanical analysis of landslides: From creeping behaviour to catastrophic failure. *G otechnique* **2015**, *66*, 202–219. [[CrossRef](#)]
191. Rice, J. Heating and weakening of faults during earthquake slip. *J. Geophys. Res.* **2006**, *111*, B5. [[CrossRef](#)]
192. Sulem, J.; Lazar, P.; Vardoulakis, I. Thermo-PoroMechanical Properties of Clayey Gouge and Application to Rapid Fault Shearing. *Int. J. Num. Anal. Meth. Geomech.* **2007**, *31*, 523–540. [[CrossRef](#)]
193. Filimonov, M.; Vaganova, N. Simulation of thermal stabilization of soil around various technical systems operating in permafrost. *Appl. Math. Sci.* **2013**, *7*, 7151–7160. [[CrossRef](#)]
194. Uzer, A. Evaluation of Freezing-Thawing Cycles for Foundation Soil Stabilization. *Soil Mech. Found. Eng.* **2016**, *53*, 202–209. [[CrossRef](#)]
195. Makusa, G.; M csik, J.; Holm, G.; Knutsson, S. Laboratory test study on the effect of freeze–thaw cycles on strength and hydraulic conductivity of high water content stabilized dredged sediments. *Can. Geotech. J.* **2016**, *53*, 1038–1045. [[CrossRef](#)]
196. Maranh , J.; Pereira, C.; Vieira, A. Thermo-Viscoplastic Subloading Soil Model for Isotropic Stress and Strain Conditions. In *Advances in Laboratory Testing and Modelling of Soils and Shales (ATMSS)*, 1st ed.; Ferrari, A., Laloui, L., Eds.; Springer International Publishing: Cham, Switzerland, 2017; pp. 405–412. ISBN 978-3-319-52773-4.
197. Hueckel, T.; Pellegrini, R. Thermoplastic modelling of undrained failure of saturated clay due to heating. *Soils Found.* **1991**, *31*, 1–16. [[CrossRef](#)]
198. Laloui, L.; Cekerevac, C. Thermo-plasticity of clays: An isotropic yield mechanism. *Comput. Geotech.* **2003**, *30*, 649–660. [[CrossRef](#)]
199. Vieira, A.; Maranh , J.R. Thermoplastic analysis of a thermoactive pile in a normally consolidated Clay. *Int. J. Geomech.* **2017**, *17*, 04016030. [[CrossRef](#)]
200. Mitchell, J.K. *Fundamentals of Soil Behavior*, 2nd ed.; Wiley InterScience: New York, NY, USA, 1993; p. 592, ISBN 978-0-471-46302-3.
201. Laloui, L.; Di Donna, A. Understanding the behaviour of energy geo-structures. In *Proceedings of the Institution of Civil Engineers ICE—Civil Engineering*; Institution of Civil Engineers: London, UK, 2011; Volume 164, pp. 184–191.
202. Bourne-Webb, P. Observed response of energy geostructures. In *Energy geostructures: Innovation in underground Engineering*; Laloui, L., Di Donna, A., Eds.; Wiley: Hoboken, NJ, USA; ISTE: London, UK, 2013; pp. 45–77, ISBN 978-1-84821-572-6.
203. Cekerevac, C. Thermal Effects on the Mechanical Behaviour of Saturated Clays: An Experimental and Constitutive Study. Ph.D. Thesis,  cole Polytechnique F d rale de Lausanne, Lausanne, Switzerland, 2003.
204. Di Donna, A.; Laloui, L. Response of soil subjected to thermal cyclic loading: Experimental and constitutive study. *Eng. Geol.* **2015**, *190*, 65–76. [[CrossRef](#)]
205. Gens, A. Soil-environment interactions in geotechnical engineering. *G otechnique* **2010**, *60*, 3–74. [[CrossRef](#)]



206. François, B.; Laloui, L. ACMEG-TS: A constitutive model for unsaturated soils under non-isothermal conditions. *Int. J. Numer. Anal. Methods Geomech.* **2008**, *32*, 1955–1988. [[CrossRef](#)]
207. Bolzon, G.; Schrefler, B. Thermal effects in partially saturated soils: A constitutive model. *Int. J. Numer. Anal. Methods Geomech.* **2005**, *29*, 861–877. [[CrossRef](#)]
208. Voight, B.; Faust, C. Frictional heat and strength loss in some rapid landslides. *Géotechnique* **1982**, *32*, 43–54. [[CrossRef](#)]
209. Vardoulakis, I. Catastrophic landslides due to frictional heating of the failure plane. *Mech. Cohesive-Frict. Mater.* **2000**, *5*, 443–467. [[CrossRef](#)]
210. Laloui, L.; Francois, B. ACMEG-T: Soil thermoplasticity model. *J. Eng. Mech.* **2009**, *135*, 932–944. [[CrossRef](#)]
211. Robinet, J.C.; Pasquiou, A.; Jullien, A.; Belanteur, N.; Plas, F. Expériences de laboratoire sur le comportement thermo-hydro-mécanique de matériaux argileux remaniés gonflants et non gonflants. *Revue Française de Géotechnique* **1997**, *81*, 53–80. [[CrossRef](#)]
212. Burghignoli, A.; Desideri, A.; Miliziano, S. A laboratory study on the thermomechanical behaviour of clayey soils. *Can. Geotech. J.* **2000**, *37*, 764–780. [[CrossRef](#)]
213. Stewart, M.A.; MacCartney, J.S. Centrifuge Modeling of Soil-Structure Interaction in Energy Foundations. *J. Geotech. Geoenviron. Eng.* **2013**, *140*. [[CrossRef](#)]
214. Graham, J.; Tanaka, N.; Crilly, T.; Alfaro, M. Modified Cam-Clay modelling of temperature effects in clays. *Can. Geotech. J.* **2001**, *38*, 608–621. [[CrossRef](#)]
215. Hueckel, T.; François, B.; Laloui, L. Explaining thermal failure in saturated clays. *Géotechnique* **2009**, *59*, 197–212. [[CrossRef](#)]
216. Abuel-Naga, M.; Bergado, T.; Bouazza, A. Thermally induced volume change and excess pore water pressure of soft Bangkok clay. *Eng. Geol.* **2007**, *89*, 144–154. [[CrossRef](#)]
217. Hueckel, T.; Pellegrini, R.; Del Olmo, C. A constitutive study of thermo-elasto-plasticity of deep carbonatic clays. *Int. J. Numer. Anal. Methods Geomech.* **1998**, *22*, 549–574. [[CrossRef](#)]
218. Baldi, G.; Hueckel, T.; Peano, A.; Pellegrini, R. *Developments in Modelling of Thermo-Hydro-Geomechanical Behaviour of Boom Clay and Clay-Based Buffer Materials*; Report 13365/2 EN; Commission of European Communities: Brussels, Belgium, 1991.
219. Towhata, I.; Kuntiwattanakul, P.; Seko, I.; Ohishi, K. Volume change of clays induced by heating as observed in consolidation tests. *Soils Found.* **1993**, *33*, 170–183. [[CrossRef](#)]
220. Plum, R.L.; Esrig, M.I. *Some Temperature Effects on Soil Compressibility and Pore Water Pressure*; Highway Research Board Special Report 103; Highway Research Board: Washington, DC, USA, 1969; pp. 231–242.
221. Demars, K.R.; Charles, R.D. Soil volume changes induced by temperature cycling. *Can. Geotech. J.* **1982**, *19*, 188–194. [[CrossRef](#)]
222. Sultan, N.; Delage, P.; Cui, Y.J. Temperature effects on the volume change behavior of Boom clay. *Eng. Geol.* **2002**, *64*, 135–145. [[CrossRef](#)]
223. Abuel-Naga, H.M.; Bergado, D.T.; Soralump, S.; Rujicpat, P. Thermal consolidation of soft Bangkok clay. *Int. J. Lowl. Technol.* **2005**, *17*, 13–22.
224. Baldi, G.; Hueckel, T.; Pellegrini, R. Thermal volume changes of the mineral-water system in low-porosity clay soils. *Can. Geotech. J.* **1988**, *25*, 807–825. [[CrossRef](#)]
225. Di Donna, A.; Ferrari, A.; Laloui, L. Experimental investigation of the soil-concrete interface: Physical mechanisms, cyclic mobilisation and behaviour at different temperatures. *Can. Geotech. J.* **2015**, *53*, 659–672. [[CrossRef](#)]
226. Marques, M.E. Influence of Strain RATE and Temperature in Natural Clays Compaction. Master's Thesis, Université Laval, Laval, QC, Canada, 1996. (In Portuguese)
227. Boudali, M.; Leroueil, S.; Srinivasa Murthy, B.R. Viscous behaviour of natural clays. In Proceedings of the 13th International Conference Soil Mechanics and Foundation Engineering ICSMFE, New Delhi, India, 5–10 January 1994.
228. Di Donna, A.; Laloui, L. Soil response under the thermo mechanical conditions imposed by energy geostructures. In *Energy Geostructures: Innovation in Underground Engineering*; Laloui, L., Di Donna, A., Eds.; Wiley: Hoboken, NJ, USA; ISTE: London, UK, 2013; pp. 45–77, ISBN 978-1-84821-572-6.
229. Laloui, L.; Cekerevac, C.; Francois, B. Constitutive modelling of the thermo-plastic behaviour of soils. *Eur. J. Environ. Civ. Eng.* **2005**, *9*, 635–650.

230. Kuntiwattanakul, P. Effect of High Temperature on Mechanical Behaviour of Clays. Ph.D. Thesis, University of Tokyo, Tokyo, Japan, 1991.
231. *Standard Test Method for Calculating Thermal Diffusivity of Rock and Soil*; ASTM D4612–16; ASTM International: West Conshohocken, PA, USA, 2016. [[CrossRef](#)]
232. Swiss Federal Office of Energy (BFE). *Innovative Improvements of Thermal Response Tests*; Final Report Project 101-690; BFE: Ittigen, Switzerland, 2008; 68p.
233. Amis, A.; Bourne-Webb, P.; Amatya, B.; Soga, K.; Davidson, C. The effects of heating and cooling energy piles under working load at Lambeth College. In Proceedings of the 33rd Annual and 11th International DFI Conference, New York, NY, USA, 15–17 October 2008.
234. Lennon, D.J.; Watt, E.; Suckling, T.P. Energy piles in Scotland. In Proceedings of the 5th International Conference on Deep Foundations on Bored and Auger Piles, Ghent, Belgium, 20 August 2008; Van Impe, W.F., Van Impe, P., Eds.; Taylor & Francis Group: London, UK, 2009.
235. Brettman, T.P.E.; Amis, T.; Kapps, M. Thermal conductivity analysis of geothermal energy piles. In Proceedings of the 2010 Geotechnical Challenges in Urban Regeneration Conference, London, UK, 26–28 May 2010.
236. Abdelaziz, S.L.A.M. Deep Energy Foundations: Geotechnical Challenges and Design Considerations. Ph.D. Thesis, Virginia Polytechnic Institute and State University, Blacksburg, Virginia, February 2013.
237. Loveridge, F.; Olgun, C.G.; Brettmann, T.; Powrie, W. The Thermal Behaviour of Three Different Auger Pressure Grouted Piles Used as Heat Exchangers. *Geotech. Geol. Eng.* **2014**, *33*, 1–17. [[CrossRef](#)]
238. Baycan, S.; Haberfield, C.; Chapman, G.; Wang, B.; Bouazza, A.; Singh, R.; Barry-Macaulay, D. Field investigation of a geothermal energy pile: Initial observations. In Proceedings of the 18th International Conference on Soil Mechanics and Geotechnical Engineering, Paris, France, 2–6 September 2013.
239. You, S.; Cheng, X.; Guo, H.; Yao, Z. In-situ experimental study of heat exchange capacity of CFG pile geothermal exchangers. *Energy Build.* **2014**, *79*, 23–31. [[CrossRef](#)]
240. Murphy, K.D.; McCartney, J.S.; Henry, K.S. Evaluation of thermo-mechanical and thermal behavior of full-scale energy foundations. *Acta Geotech.* **2014**, *10*, 179–195. [[CrossRef](#)]
241. Yu, K.; Singh, R.; Bouazza, A.; Bui, H. Determining soil thermal conductivity through numerical simulation of a heating test on a heat exchanger pile. *Geotech. Geol. Eng.* **2015**, *33*, 239–252. [[CrossRef](#)]
242. Carlsson, S. Energipålar-Termiskt Responstest på Prefabricerad Energipåle i Betong. Master's Thesis, Lund University, Lund, Sweden, 2015.
243. Ronchi, F.; Salciarini, D.; Cavalagli, N.; Tamagnini, C. Numerical Model of Energy Foundation Behavior: The Prototype of a Geothermal Micro-pile. *Procedia Eng.* **2016**, *158*, 326–331. [[CrossRef](#)]
244. Middleton, M.F. A transient method of measuring the thermal properties of rocks. *Geophysics* **1993**, *58*, 357–365. [[CrossRef](#)]

